

UC Berkeley

UC Berkeley Previously Published Works

Title

The Relationship Between African Easterly Waves and Tropical Cyclones in Historical and Future Climates in the HighResMIP-PRIMAVERA Simulations

Permalink

<https://escholarship.org/uc/item/0p2158k2>

Journal

Journal of Geophysical Research: Atmospheres, 128(7)

ISSN

2169-897X

Authors

Bercos-Hickey, Emily
Patricola, Christina M
Loring, Burlen
et al.

Publication Date

2023-04-16

DOI

10.1029/2022jd037471

Copyright Information

This work is made available under the terms of a Creative Commons Attribution License, available at <https://creativecommons.org/licenses/by/4.0/>

Peer reviewed



RESEARCH ARTICLE

10.1029/2022JD037471

Key Points:

- Future changes in the frequency of African easterly waves (AEWs) are not a good indicator of future tropical cyclone (TC) activity
- AEWs that develop into TCs are stronger than non-developing waves in historical and future climates
- Wave strength combined with environmental conditions are good indicators of tropical cyclogenesis from waves

Correspondence to:

E. Bercos-Hickey,
ebercoshickey@lbl.gov

Citation:

Bercos-Hickey, E., Patricola, C. M., Loring, B., & Collins, W. D. (2023). The relationship between African easterly waves and tropical cyclones in historical and future climates in the HighResMIP-PRIMAVERA simulations. *Journal of Geophysical Research: Atmospheres*, 128, e2022JD037471. <https://doi.org/10.1029/2022JD037471>

Received 13 JUL 2022
Accepted 28 MAR 2023

Author Contributions:

Conceptualization: Emily Bercos-Hickey
Data curation: William D. Collins
Formal analysis: Emily Bercos-Hickey
Methodology: Christina M. Patricola
Software: Burlen Loring
Visualization: Emily Bercos-Hickey
Writing – original draft: Emily Bercos-Hickey
Writing – review & editing: Christina M. Patricola

The Relationship Between African Easterly Waves and Tropical Cyclones in Historical and Future Climates in the HighResMIP-PRIMAVERA Simulations

Emily Bercos-Hickey¹ , Christina M. Patricola^{1,2} , Burlen Loring³ , and William D. Collins^{1,4} 

¹Climate and Ecosystem Sciences Division, Lawrence Berkeley National Laboratory, Berkeley, CA, USA, ²Department of Geological and Atmospheric Sciences, Iowa State University, Ames, IA, USA, ³Computational Sciences Division, Lawrence Berkeley National Lab, Berkeley, CA, USA, ⁴Department of Earth and Planetary Science, University of California, Berkeley, Berkeley, CA, USA

Abstract The deadly and destructive nature of tropical cyclones (TCs) makes understanding their response to future climate change of the utmost importance. TC genesis hinges on multiple factors, including an initial disturbance. African easterly waves (AEWs) have been shown to serve as such disturbances for TCs developing in the North Atlantic. It is therefore crucial to understand the relationship between AEWs and TCs and how this relationship may be affected by climate change. In this study, we examine the AEW-TC relationship in historical and future climates using three models from the HighResMIP PRIMAVERA simulations. The AEWs and TCs were tracked in the model data using objective tracking algorithms, and AEW and TC tracks were then matched together if they were close to each other in space and time. The strength of the AEWs was measured using the eddy kinetic energy and the curvature vorticity of the waves. TC strength and intensity were measured using potential intensity and lifetime maximum 10 m windspeed. We found that future changes in the frequency of AEWs are not a good indicator of future TC activity. However, AEW strength, as well as environmental conditions conducive to strong TCs, are good indicators of AEWs that develop into TCs in both historical and future climates.

Plain Language Summary Tropical cyclones (TCs) are both deadly and destructive and it is important to understand how they will respond to future climate change. African easterly waves (AEWs) are disturbances that can develop into TCs that form in the North Atlantic. The relationship between AEWs and TCs is an important part of understanding how TCs will be affected by climate change. In this study, we examine the AEW-TC relationship in historical and future climates using three climate models. AEWs and TCs were tracked in the model data, and AEW and TC tracks were then matched together if they were close to each other in space and time. The number of AEWs and TCs in the historical and future climates were compared. We found that future changes in the number of AEWs are not a good indicator of future changes in the number of TCs. However, AEW strength, as well as environmental conditions conducive to strong TCs, are good indicators of AEWs that develop into TCs in both historical and future climates.

1. Introduction

Tropical cyclones (TCs) and their associated heavy precipitation, high winds, and storm surges are both deadly and destructive, leading to losses in the United States that can often exceed \$1 billion for an individual event (Cerveny et al., 2017; NOAA, 2021; Yue et al., 2012). The genesis of these extreme events hinges on the co-occurrence of multiple environmental factors, including warm sea surface temperatures (SSTs), a moist mid-troposphere, weak vertical wind shear, and an initial precursor or “seed” disturbance (Avila, 1991; Emanuel, 1988; Frank & Ritchie, 2001; Gray, 1968; Landsea, 1993). In the Atlantic basin, African easterly waves (AEWs) have been shown to serve as the seeds that can precede TC genesis (Avila & Pasch, 1992; Landsea, 1993). AEWs are synoptic-scale disturbances that propagate along the African easterly jet (AEJ) in two tracks north and south of ~15°N and grow off of the baroclinic-barotropic instability of the AEJ (Burpee, 1972; Pytharoulis & Thorncroft, 1999). Recently, the relationship between AEWs and TCs has been called into question, with regional climate model data indicating that suppressed AEW activity did not affect basin-wide Atlantic TC frequency (Danso et al., 2022; Patricola et al., 2018). The AEW-TC relationship is further complicated by the potential effects of anthropogenic climate change, where studies have shown that climate change may double the economic damages of TCs by the year 2100

© 2023. The Authors.

This is an open access article under the terms of the [Creative Commons Attribution License](https://creativecommons.org/licenses/by/4.0/), which permits use, distribution and reproduction in any medium, provided the original work is properly cited.

through increased TC intensity, precipitation, and storm surge (Knutson et al., 2020; Mendelsohn et al., 2012; Patricola & Wehner, 2018). It is therefore crucial to develop a better understanding of the AEW-TC relationship given the potentially devastating impacts of future climate change.

The relationship between AEWs and TCs has been examined in both observational and modeling studies (Avila & Pasch, 1992; Caron & Jones, 2012; Frank, 1970; Hopsch et al., 2009; Landsea, 1993; Patricola et al., 2018; Russell et al., 2017; Thorncroft & Hodges, 2001). Some studies have found a strong relationship between TC genesis and AEW activity. For example, observational and reanalysis data have been used to show that approximately 60% of TCs and 85% of major hurricanes develop from AEWs (Frank, 1970; Landsea, 1993; Russell et al., 2017). Thorncroft and Hodges (2001) and Hopsch et al. (2007) used reanalysis data and an AEW tracking algorithm to examine the AEW-TC relationship. Thorncroft and Hodges (2001) found that tracked AEWs were positively correlated with Atlantic TC activity between 1985 and 1998 and that TC activity was mostly associated with the southern AEW track. Hopsch et al. (2007) found a significant positive correlation between the 2–6 day filtered meridional wind and Atlantic TC activity, although tracked AEWs and TC activity were not correlated between 1952 and 2002. As an alternative to tracking algorithms, Russell et al. (2017) used eddy kinetic energy (EKE) to estimate AEW activity. They found a correlation between seasonal mean EKE in the lower troposphere equatorward of the southern AEW track and TC genesis, suggesting that the low-level circulation associated with AEWs exerts more control over TC genesis than mid-tropospheric AEW activity (Russell et al., 2017).

Other studies have found that large-scale environmental conditions are a stronger control than TC seeds on TC genesis (Caron & Jones, 2012; Danso et al., 2022; Emanuel, 2022; Hoogewind et al., 2020; Patricola et al., 2018). Caron and Jones (2012) used a regional climate model to examine the effects of lateral boundary conditions and domain size on AEWs and TCs. Across all simulations, they concluded that the large-scale atmospheric environment was the primary control of simulated TC activity. AEW activity was not sufficient to predict Atlantic TC numbers (Caron & Jones, 2012). Similarly, Emanuel (2022) found that climatological TC frequency is controlled primarily by environmental conditions and Hoogewind et al. (2020) found that the spatiotemporal distribution of favorable environmental conditions strongly modulates the seasonal cycle of TCs. Patricola et al. (2018) and Danso et al. (2022) used a regional climate model to examine the AEW-TC relationship by comparing ensembles of simulations where AEWs were either prescribed or removed through the lateral boundary conditions. Both studies found that suppressed AEW activity did not affect basin-wide Atlantic TC frequency (Danso et al., 2022; Patricola et al., 2018).

The lack of agreement among research on the AEW-TC relationship may in part stem from the disproportionate number of AEWs and TCs in the Atlantic basin each hurricane season. Studies have shown that only about 15%–20% of AEWs develop into TCs (Dunkerton et al., 2009; Frank, 1970), and, as stated above, not every TC develops from an AEW. Previous research has aimed to better understand why some AEWs do or do not develop into TCs (Agudelo et al., 2011; Hopsch et al., 2009; Satoh et al., 2013), referred to as “developing” and “non-developing” AEWs, respectively. Hopsch et al. (2009) used reanalysis data to examine the characteristics, lifecycles, and environments of developing and non-developing AEWs. They found that developing AEWs have larger amplitudes and that convection is maintained in the trough of developing waves as they move from Africa out into the Atlantic Ocean. Additionally, SSTs were warmer for the developing AEWs, suggesting that environmental conditions cannot be ruled out for TC genesis (Hopsch et al., 2009). Agudelo et al. (2011) developed a Bayesian diagnostic method to better understand the genesis of North Atlantic TCs spawned by AEWs. Similar to Hopsch et al. (2009), Agudelo et al. (2011) found that large amplitude AEWs as well as convectively coupled waves were more likely to spawn TCs. TC genesis also increased when the AEWs entered an environment of pre-existing moist convection (Agudelo et al., 2011). Satoh et al. (2013) used a decade of reanalysis data to examine the differences between developing and non-developing AEWs. They found that mid-level humidity associated with AEWs was related to TC genesis location and that developing AEWs had a more northern-oriented wave train than non-developing waves (Satoh et al., 2013). In all three of the aforementioned studies, dry mid-to-upper-level air ahead of an AEW is noted as a major limitation for wave development.

A complicating factor in understanding the AEW-TC relationship is the potential effect of climate change. Studies have examined how climate change will affect both AEWs (Bercos-Hickey & Patricola, 2021; Brannan & Martin, 2019; Hannah & Ayyer, 2017; Kebe et al., 2020; Martin & Thorncroft, 2015; Skinner & Dickenbaugh, 2014) and TCs (Grossmann & Morgan, 2011; Knutson et al., 2010, 2020; Patricola & Wehner, 2018; Sobel et al., 2016; Walsh et al., 2016; Wehner et al., 2018). Of the studies that have examined AEWs, results are conflicting. Skinner

and Diffenbaugh (2014), Martin and Thorncroft (2015), and Brannan and Martin (2019) used global climate model (GCM) data to show a future increase in AEW activity in the northern track, while changes in the southern track remained inconclusive, largely owing to poor model resolution of the Guinea Highlands. Hannah and Aiyer (2017) used a superparameterized GCM to examine the response of AEWs to quadrupled CO₂ concentrations. They found increased AEW activity in the northern track due to enhanced baroclinicity, and decreased activity in the southern track, which was attributed to weak temperature gradient balance. Kebe et al. (2020) used a regional climate model to examine the response of the AEJ and AEWs to climate change. In contrast to the previous studies, Kebe et al. (2020) found a future decrease in AEW activity and an overall decrease in favorable conditions for AEW growth due to a reduction in barotropic and baroclinic instability. Bercos-Hickey and Patricola (2021), however, also used a regional climate model to examine the effects of climate change on the AEJ and AEWs and they found a future increase in both the number and strength of AEWs. The disagreement between the above studies could be due, in part, to the differences in tracking methods, models, and model resolution. The conflicting results, however, highlight the uncertainty in how AEWs will respond to future climate change.

The response of TCs to climate change also remains uncertain, with no theory to explain global TC number (Sobel et al., 2021). In their summary paper, Knutson et al. (2020) reported that there is less agreement and lower confidence on the effects of climate change on TC frequency. Some studies have found a future decrease in TC frequency (Gualdi et al., 2008; Knutson et al., 2008, 2010; Tory et al., 2013; Wehner et al., 2015, 2018), while other studies have found a future increase (Bhatia et al., 2018; Emanuel, 2013). The proportion of category 4–5 TCs, however, is projected to increase with future climate change (Bender et al., 2010; Holland & Bruyère, 2014; Knutson et al., 2020). There is greater consensus and higher confidence on the effects of climate change on TC intensity, precipitation rates, and storm surge. Future climate change is projected to increase TC intensity, with a median increase in lifetime maximum surface wind speeds of 5% for a 2°C global warming (Emanuel, 1987; Hill & Lackmann, 2011; Knutson et al., 2020; Knutson & Tuleya, 2004; Patricola & Wehner, 2018). TC-related precipitation is also projected to increase, with increases in near-storm precipitation rates at least as large as the Clausius–Clapeyron limit of 7% increase given anthropogenic warming of 1°C (Knutson et al., 2020; Patricola & Wehner, 2018; Risser & Wehner, 2017; Scoccimarro et al., 2014; Villarini et al., 2014; Wright et al., 2015). Additionally, studies have shown that future sea level rise will, for the most part, lead to an increase in TC storm surge (Garner et al., 2017; Knutson et al., 2020; Little et al., 2015).

To better understand the future of TC genesis, recent studies have examined the response of TC seeds to climate change, where TC seeds are defined as pre-TC synoptic scale disturbances (Hsieh et al., 2020, 2022; Sugi et al., 2020; Vecchi et al., 2019; Yamada et al., 2021). In these studies, the effects of climate change on TC seeds, which are not limited to AEWs, and the seed-TC relationship are unclear. Vecchi et al. (2019) used GCMs of varying horizontal resolutions to examine the response of TCs and TC seeds to CO₂ doubling and surface warming. They found that seed disturbances were the main driver of TC frequency; changes in TC frequency were controlled by changes in the frequency of TC seeds and the probability that each seed developed. However, the response of TC seeds to climate change was inconsistent, with seeds increasing due to surface warming but decreasing due to higher CO₂ (Vecchi et al., 2019). Hsieh et al. (2020) and Hsieh et al. (2022) also used model data to examine the response of TCs to increased CO₂ and surface warming. Hsieh et al. (2020) found that with uniform surface warming and CO₂ doubling, the response of TCs can be attributed to the response of TC seeds. In patterned warming experiments, the TC response did not always follow the seed response, which was likely due to changes in the ventilation index that affected seed development (Hsieh et al., 2020). Building on previous TC seed research (Hsieh et al., 2020; Yang et al., 2021), Hsieh et al. (2022) examined GCM experiments and found that seed frequency strongly influences TC frequency across climate perturbations. Similar to Vecchi et al. (2019), Hsieh et al. (2020) and Hsieh et al. (2022), Sugi et al. (2020) used high resolution GCM data to examine future changes in TC and TC seed frequency. They found a future decrease in the number of TC seeds and weak (category 2 or less) TCs, but they also found a future increase in the most intense (category 5) TCs. Yamada et al. (2021), however, used a multi-model ensemble mean from high resolution GCM data and found a significant future decrease in TC genesis frequency, which they attributed to changes in TC seeds. The lack of consensus on the future of TC seeds and their relationship with TC genesis in the aforementioned studies further demonstrates the diversity of TC and AEW projections across different models and future climate scenarios.

There has been an extensive amount of research on AEWs and TCs regarding their relationship and how they will respond to climate change. However, critical knowledge gaps and uncertainty remain. Studies have found conflicting results on the response of both AEWs (Bercos-Hickey & Patricola, 2021; Brannan & Martin, 2019;

Table 1
Three GCMs From the HighResMIP PRIMAVERA Simulations and Their Characteristics

Model	EC-Earth3P	CMCC-CM2	HadGEM3-GC3.1
High resolution name	HR	VHR4	HM
Atmospheric mesh spacing (km) at 0°N	39	28	39
Atmospheric mesh spacing (km) at 50°N	36	18	25
Atmospheric nominal resolution (km) in CMIP6	50	25	50
Atmospheric model levels	91	26	85
Ocean resolution (degrees)	0.25	0.25	0.08

Kebe et al., 2020) and TCs to climate change (Bhatia et al., 2018; Tory et al., 2013; Wehner et al., 2015, 2018). The relationship between AEWs and TCs is also not completely clear, with some studies finding a connection between the two (Hopsch et al., 2009; Landsea, 1993; Russell et al., 2017), but more recent work calling this relationship into question (Danso et al., 2022; Patricola et al., 2018). In this study, our objective is to better understand the AEW-TC relationship and how it may be affected by future climate change. What are the characteristics and environments of developing AEWs and TCs that develop from AEWs? Do future changes in AEWs translate to future changes in TCs? To address these questions, we use high resolution GCM data to examine AEWs and TCs in historical and future climate scenarios. The models and methods used in this study are presented in Section 2, while the results are presented in Sections 3–5. The conclusions are presented in Section 6.

2. Models and Methods

The climate model simulations used in this study are from the High-Resolution Model Intercomparison Project (HighResMIP) (Haarsma et al., 2016), which is endorsed by the Coupled Model Intercomparison Project Phase 6 (CMIP6). Three HighResMIP PRIMAVERA models were used in the analysis, as shown in Table 1. The three models, EC-Earth3P (Haarsma et al., 2020), CMCC-CM2 (Cherchi et al., 2019), and HadGEM3-GC3.1 (Roberts et al., 2019), were chosen because of data availability in the archive. The multi-model ensemble used in this study was produced by the European Union Horizon 2020 project PRIMAVERA, which ran simulations following the HighResMIP protocol at high horizontal resolution (25–50 km) as well as at the standard CMIP6 horizontal resolution (100 km) (Roberts et al., 2020a). Simulations were run for the three models from 1950 to 2050, where the years 1950–2014 are the historical period and the years 2015–2050 are the future period. Model frequency was 6-hourly for EC-Earth3P and CMCC-CM2 and 3-hourly for HadGEM3-GC3.1. For the purpose of our analysis, and for the remainder of the paper (unless otherwise stated), we define the historical period as 1950–1980 and the future period as 2020–2050, as in Roberts et al. (2020b).

Both atmosphere-only (uncoupled) and atmosphere-ocean coupled simulations were produced by the EC-Earth3P, CMCC-CM2, and HadGEM3-GC3.1 models. In the historical (1950–2014) atmosphere-only simulations, SSTs and sea ice were prescribed from the daily $0.25^\circ \times 0.25^\circ$ resolution Hadley Centre Global Sea Ice and SST data set (Kennedy et al., 2017). In the future (2015–2050) atmosphere-only simulations, SST and sea ice forcings were constructed by imposing future warming estimates from the CMIP5 Representative Concentration Pathway 8.5 (Meinshausen et al., 2011) simulations on historical SST and sea ice (Haarsma et al., 2016). In the atmosphere-ocean coupled simulations, model spin-up was produced using a 50-year integration starting at 1950 and using 1950 forcings. The model integration was then continued for the period 1950–2050 with a fully coupled atmosphere and ocean (Haarsma et al., 2016).

We tracked simulated AEWs in the EC-Earth3P, CMCC-CM2, and HadGEM3-GC3.1 models as in Bercos-Hickey and Patricola (2021), who used a modified version of the objective tracking algorithm from Brammer and Thorncroft (2015). Although tracking algorithms are inherently sensitive to parameter tuning, this algorithm has been used with both reanalysis and model data and produces AEW counts that are in good agreement with the observational record (Bercos-Hickey & Patricola, 2021; Brammer & Thorncroft, 2015, 2017; Brannan & Martin, 2019), lending confidence to its use in this study. The tracking algorithm utilizes curvature vorticity (CV) maxima at 700 hPa, which have been shown to distinguish the trough of a wave from the background shear vorticity and removes any bias associated with the strength of the AEJ (Bain et al., 2014; Berry et al., 2007).

The locations of unique CV maxima are determined at each time step and relative vorticity maxima are used to fine tune these locations. The maxima are then advected using the stream function to find the next point in time, and the locations of the advected maxima are corrected through a comparison with the unique CV maxima at the next time step. As in Brammer and Thorncroft (2015), a magnitude-weighted centroid is calculated to select the CV centroid if multiple weak CV maxima are present. Consistent with Bercos-Hickey and Patricola (2021), the algorithm considers CV maxima to have magnitudes greater than or equal to $0.2 \times 10^{-5} \text{ s}^{-1}$. To ensure that only well-developed waves are retained by the algorithm and to be consistent with previous research, tracked AEWs are only kept if they last for more than 2 days, travel more than 15° of longitude, and exist east of 5°W and west of 20°W (Bercos-Hickey & Patricola, 2021; Brammer & Thorncroft, 2015; Brannan & Martin, 2019).

Simulated TCs were objectively tracked in the EC-Earth3P, CMCC-CM2, and HadGEM3-GC3.1 models. Objectively tracked TCs are sensitive to the choice of tracking algorithm, as well as the metrics used within the trackers (Bourdin et al., 2022; Zarzycki & Ullrich, 2017). Intensity thresholds in particular have been shown to drive differences in TC frequencies between trackers (Horn et al., 2014). Here we use the feature-tracking algorithm TRACK (Hodges et al., 2017) to remain consistent with previous HighResMIP TC research (Roberts et al., 2020a, 2020b). The TRACK algorithm uses 6-hourly relative vorticity at the levels 850, 700, and 600 hPa, vertically averaged, as its primary feature-tracking variable, but also uses warm-core and TC lifetime as criteria. The TRACK algorithm operates by transforming each model output to a common T63 spectral grid where spectral filtering is used to remove noise from the smallest spatial scales in the vorticity. The algorithm then identifies vorticity maxima, defined by exceedances of $5 \times 10^{-6} \text{ s}^{-1}$, at each time step and links the maxima together using a nearest neighbor approach (Hodges et al., 2017). Further refinement involves retaining only tracks that last at least 2 days and isolating tracks that are warm-core TCs. The characteristics of the HighResMIP TC tracks from the TRACK algorithm have been summarized in previous research (Roberts et al., 2020a, 2020b). For the purposes of this research, we are only interested in North Atlantic TCs. Therefore only TCs in the North Atlantic are retained, which is defined as in Roberts et al. (2020a, 2020b), but with the eastern edge extended from 20°W to 15°W .

To determine if an AEW develops into a TC, we ran a program that connected AEW and TC tracks in time and space. To connect AEWs and TCs, we found points along the AEW and TC tracks that were within 1 day and 1,000 km of each other. This buffer in time and space was chosen to account for the fact that the AEW and TC tracks are recorded as a connection of single latitude and longitude points in time, whereas in reality these disturbances are much larger than single points. Throughout the remainder of the paper, we consider AEW tracks that connect with TC tracks as developing waves, and AEWs that do not have a connecting TC as non-developing waves. Similarly, the corresponding TCs are considered as either developing from an AEW or not developing from an AEW.

AEW strength was assessed in the EC-Earth3P, CMCC-CM2, and HadGEM3-GC3.1 models using the EKE. To isolate the AEWs in the EKE calculations, the perturbations in the zonal and meridional wind were temporally filtered for 2–6 days using a bandpass filter, consistent with previous research (Bercos-Hickey et al., 2022; Hopsch et al., 2009). TC strength was assessed using the potential intensity (PI) (Emanuel, 1986, 1988), as PI provides an upper bound on the maximum intensity of TCs. To calculate PI, we utilized the Toolkit for Extreme Climate Analysis (Loring et al., 2016), which allowed for the computationally intensive calculations using parallel processing across the time dimension at each grid point within the model domains. The surface temperature, which is needed for the PI calculations, was missing from the HadGEM3-GC3.1 model. To circumvent this issue, we derived the surface temperature from the longwave surface radiation using the Stefan-Boltzmann law. In the following sections, the EKE for developing (non-developing) waves is calculated using the time-averaged EKE that only includes all times of developing (non-developing) waves between May–November at each grid point. Similarly, the PI for TCs that develop (do not develop) from AEWs is calculated using the time-averaged PI that only includes all times of TCs that develop (do not develop) from AEWs between May–November at each grid point. We found that the developing and non-developing datasets were sufficiently independent that this averaging method provided meaningful results.

3. African Easterly Wave and Tropical Cyclone Tracks

We begin our analysis by examining the AEWs and North Atlantic TCs in the EC-Earth3P, CMCC-CM2, and HadGEM3-GC3.1 models. Table 2 shows the average number of AEW and TC tracks from May–November

Table 2

Average Number of May–November African Easterly Waves and Tropical Cyclones From 1950–1980 (Historical) and 2020–2050 (Future) and the Percent Change Between the Historical and Future Climates of the Coupled and Uncoupled Simulations of the Three HighResMIP Models

	EC-Earth3p-HR		CMCC-CM2-VHR4		HadGEM3-GC31-HM	
	AEWs	TCs	AEWs	TCs	AEWs	TCs
Historical coupled	43	5	68	2	54	16
Future coupled	48	4	66	3	51	14
Percent change	12	−20	−3	50	−6	−13
<i>p</i> -value	0.001	0.01	0.3	0.2	0.1	0.07
Historical uncoupled	39	5	61	11	57	19
Future uncoupled	40	5	55	9	62	19
Percent change	3	0	−10	−18	9	0
<i>p</i> -value	0.6	0.5	0.004	0.02	0.02	0.9

Note. *P*-values correspond to *t*-tests for differences between the means of the historical and future simulations.

between 1950–1980 and 2020–2050 for the coupled and uncoupled simulations of the three models. To demonstrate the interannual spread of the track counts in the historical and future time periods, Figure 1 shows boxplots of the average May–November AEW and North Atlantic TC track counts between 1950–1980 and 2020–2050 for all simulations of the three models. Previous studies have found that the observed number of AEWs per season can range from in the twenties to the fifties (Bain et al., 2014; Bercos-Hickey & Patricola, 2021; Brannan & Martin, 2019; Fink & Reiner, 2003; Hopsch et al., 2009; Thorncroft & Hodges, 2001). Table 2 and Figure 1 indicate that the number of AEWs in the three HighResMIP models is mostly in good agreement with observed counts from previous research, although some simulations, such as the coupled CMCC-CM2, have counts in the sixties. This is not necessarily surprising given that in this study the season is from May–November, as in Roberts et al. (2020b), whereas previous AEW studies have typically used the season May–October (Bercos-Hickey & Patricola, 2021). In contrast, Table 2 and Figure 1 indicate that the number of simulated TCs is low, more so in the coupled simulations and in the EC-Earth3P and CMCC-CM2 models, when compared to the long-term mean of 9.2 North Atlantic TCs per season from the 1900–2006 record (Landsea, 2007). This lower frequency of North Atlantic TCs was also noted by Roberts et al. (2020a), and is likely due to ongoing challenges in simulating North Atlantic TCs, possibly due to low rates of intensification as well as sensitivity to model physics and SST biases in the coupled simulations (Camargo, 2013; Chauvin et al., 2020; Manganello et al., 2012; Roberts et al., 2020b).

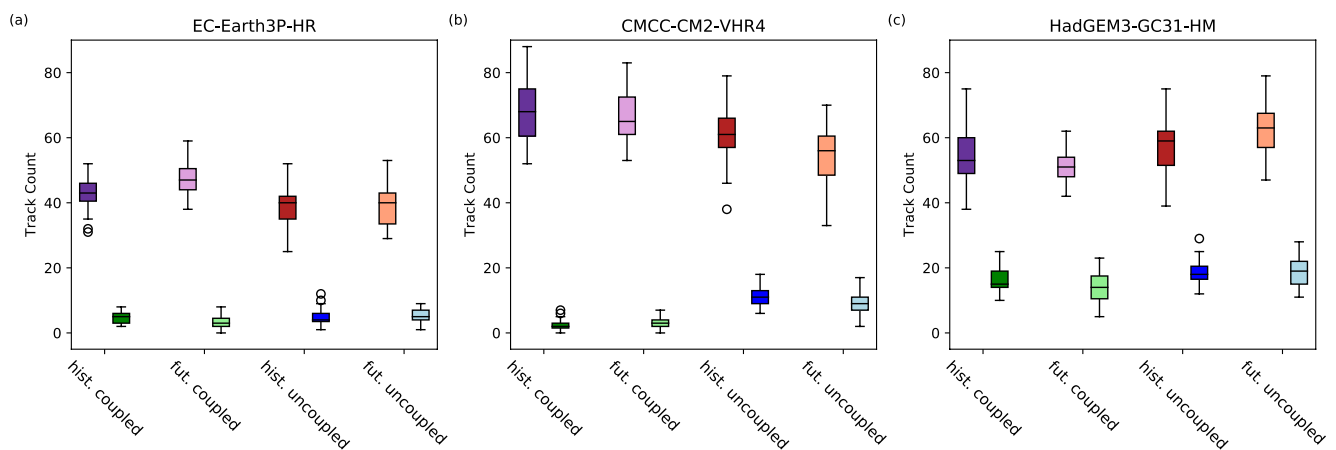


Figure 1. Boxplots of African easterly wave (purple and red) and tropical cyclone (green and blue) track counts from the historical and future coupled and uncoupled simulations of the (a) EC-Earth3P-HR, (b) CMCC-CM2-VHR4, and (c) HadGEM3-GC31-HM models. Track counts are from May–November 1950–1980 (historical) and 2020–2050 (future). Each box shows the interquartile range (IQR) from the first quartile (Q1) to the third quartile (Q3), where the horizontal line represents the median. The whiskers of the box extend from $Q1 + 1.5 \cdot IQR$ to $Q3 - 1.5 \cdot IQR$.

Table 3
Percent of African Easterly Waves (AEWs) That Develop Into Tropical Cyclones (TCs) and the Percent of TCs That Develop From AEWs Averaged From 1950–1980 (Historical) or 2020–2050 (Future) for the Coupled and Uncoupled Simulations of the Three HighResMIP Models

	EC-Earth3p-HR		CMCC-CM2-VHR4		HadGEM3-GC31-HM	
	AEW %	TC %	AEWs %	TCs %	AEWs %	TCs %
Historical coupled	3	27	1	30	8	28
Future coupled	2	29	1	23	6	20
<i>p</i> -value	0.2	0.6	0.9	0.2	0.002	0.03
Historical uncoupled	2	17	6	30	8	25
Future uncoupled	3	20	3	19	9	30
<i>p</i> -value	0.4	0.3	0.002	0.01	0.7	0.1

Note. *P*-values correspond to *t*-tests for differences between the means of the historical and future simulations.

Additionally, Roberts et al. (2020a) found that the models struggled to achieve storm intensities greater than category 2–3, which is not surprising given that high wind speeds are beyond the expected capabilities of models at 25–50 km horizontal resolution (Davis, 2018).

Figure 1 and Table 2 show a large disagreement among the three models on the sign of the change in the number of AEWs and TCs from present to future, with the future change in AEWs and TCs having opposite signs in some simulations. For example, the coupled EC-Earth3P model indicates a future increase in AEWs and a future decrease in TCs. In contrast, the coupled CMCC-CM2 model indicates a future decrease in AEWs and a future increase in TCs, while the coupled HadGEM3-GC3.1 model indicates a future decrease in both AEWs and TCs. The AEW and TC track counts also show disagreement in the coupled versus uncoupled simulations. For example, the uncoupled HadGEM3-GC3.1 model indicates a future increase in AEWs and no change in TCs, which contradicts the results from the coupled simulations. The disagreement on future changes in TC frequency between the coupled and uncoupled simulations likely stems from differences in the SST patterns rather than the ocean wake effect (Yoshida et al., 2017). Significance testing further underscores the uncertainty in future changes in AEW and TC track counts. There is a significant difference ($p < 0.05$) between the historical and future AEW and TC track counts in some, but not all of the simulations shown in Table 2, which adds to the uncertainty in how climate change will affect the frequency of AEWs and TCs. There is also a much larger spread in AEW track counts when compared with TC counts (Figure 1), which suggests that interannual variability may have a larger effect on interpreting future changes of AEW frequency. The contradictory nature of these results is not necessarily surprising, as previous research has shown that there is large disagreement about the future of AEWs and TCs (Bercos-Hickey & Patricola, 2021; Bhatia et al., 2018; Emanuel, 2013; Gualdi et al., 2008; Kebe et al., 2020; Knutson et al., 2008, 2010; Tory et al., 2013; Wehner et al., 2015, 2018).

To examine the relationship between the AEWs and TCs in the EC-Earth3P, CMCC-CM2, and HadGEM3-GC3.1 models, we ran a program that found wave and TC tracks that were well-matched in both time and space (see Section 2). The results are presented in Table 3, which shows the average percent of AEWs that develop into TCs and the average percent of TCs that develop from AEWs for each model and experiment type. From Table 3, less than 10% of AEWs develop into TCs across all simulations, with the largest number of developing waves in the HadGEM3-GC3.1 model. Previous research has suggested that 15%–20% of AEWs develop into TCs (Dunkerton et al., 2009; Frank, 1970), which is notably higher than in this study. As discussed above, a low frequency of North Atlantic TCs was simulated by the models (Roberts et al., 2020a), leading to a low number of TC tracks. The low number of TC tracks limits the number of potential AEW-TC matches, and therefore results in a low percent of developing AEWs. Table 3 shows that about 20%–30% of TCs develop from AEWs across all simulations. Previous research has shown that approximately 60% of TCs develop from AEWs (Frank, 1970; Landsea, 1993), however this number is from observational data. The data used in this study are at a coarser resolution than observational data. Research has shown that intense TCs are more likely to have developed from AEWs (Avila & Pasch, 1992; Landsea, 1993), but the models used in this study are not high enough resolution to capture the most intense TCs (Roberts et al., 2020a). We would therefore expect a lower percent of TCs that develop from AEWs due to the reduction or lack of intense TCs in the model simulations. The low frequency of

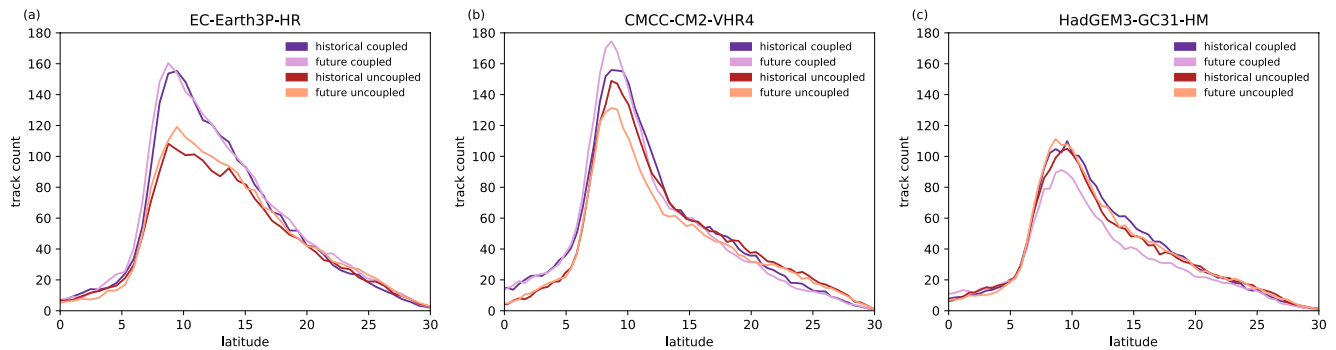


Figure 2. African easterly wave track count per 1 degree of longitude in the (a) EC-Earth3P-HR, (b) CMCC-CM2-VHR4, and (c) HadGEM3-GC3.1-HM models. Track counts are from the entire May–November 1950–1980 (historical) or 2020–2050 (future) time periods. The track counts were normalized by the number of years in each simulation.

North Atlantic TCs in the EC-Earth3P and CMCC-CM2 models also reduces the number of potential AEW-TC matches.

The results presented in Table 3 also demonstrate a large amount of variability across the three models, similar to Table 2. For example, the coupled CMCC-CM2 and HadGEM3-GC3.1 models both show a future decrease in the percent of TCs that develop from AEWs, whereas the EC-Earth3P model shows a future increase. There is also disagreement across the models on the effects of coupling, with coupling resulting in both increases and decreases in the percent of developing AEWs and developed TCs when compared to the uncoupled simulations. Significance testing further underscores the uncertainty in future changes to developing AEWs and developed TCs. There is a significant difference ($p < 0.05$) between the historical and future development percents in some, but not all of the simulations shown in Table 3, indicating that future changes in the percent of developing AEWs and developed TCs are unclear. A comparison of Tables 2 and 3 reveals that the sign of the change in the total number of AEWs and TCs from the historical to the future climate in the coupled and uncoupled simulations does not necessarily align with the change in the percent of developing waves or developed storms. For example, Table 2 indicates a future increase in AEWs for the coupled EC-Earth3P model. However, Table 3 indicates a future decrease in the percent of developing AEWs from the same model simulation. These results indicate that future changes in the frequency of AEWs and TCs do not necessarily dictate future changes in AEWs that develop into TCs. Additionally, there is a large amount of disagreement among the models on how future climate change will affect the percent of developing AEWs and TCs that develop from AEWs. This suggests a high amount of uncertainty in how future changes in the frequency of AEWs may affect future changes in TCs.

4. African Easterly Waves

In this section, we examine the May–November characteristics of the AEWs in the three HighResMIP models. We then specifically look at the differences between the developing and non-developing AEWs.

4.1. AEW Characteristics

Figure 2 shows the latitudinal locations of the AEWs in the EC-Earth3P, CMCC-CM2, and HadGEM3-GC3.1 models for the historical and future scenarios in the coupled and uncoupled simulations. The latitudinal locations shown in Figure 2 are determined by calculating the track count per 1° of longitude. Figure 2 indicates that the region between 5° and 15°N has the highest concentration of AEWs in the present and future climates and both model coupling configurations of all three models. This latitudinal band corresponds to the location of the southern AEW track and the high concentration of AEW tracks found there is consistent with previous research (Brammer & Thorncroft, 2015). Figure 2 also shows that there is little change in the latitudinal location of the AEWs between the different models and scenarios. There is, however, a clear difference in the total number of AEW tracks between the three models. The EC-Earth3P (Figure 2a) and CMCC-CM2 (Figure 2b) models have a similar number of AEW tracks across all scenarios, whereas the HadGEM3-GC3.1 model (Figure 2c) has fewer AEW tracks in all scenarios compared with the other two models and the tracks counts across all scenarios are

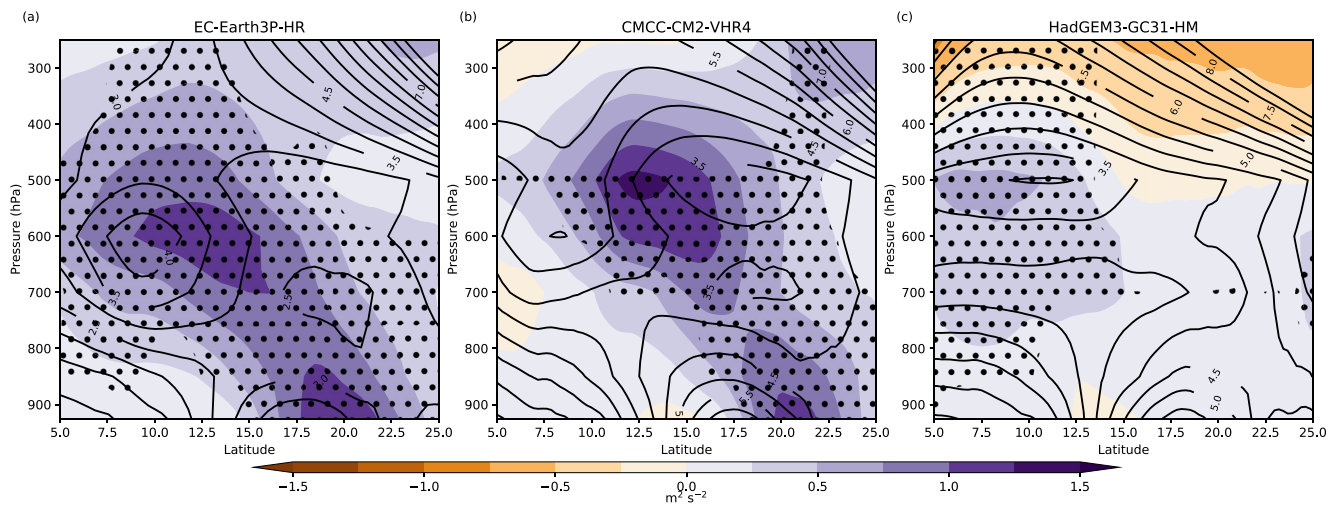


Figure 3. Eddy kinetic energy (EKE) ($\text{m}^2 \text{s}^{-2}$) zonally averaged between 20°W and 20°E from the time-averaged coupled May–November 2020–2050 (future) minus the 1950–1980 (historical) for the (a) EC-Earth3P-HR, (b) CMCC-CM2-VHR4, and (c) HadGEM3-GC3.1-HM models. Black contour lines show the historical EKE. Time averages only include times where waves occur. Stippling refers to a significant difference in EKE between the future and historical coupled simulations using a grid-cell specific two sample t -test with the p -values adjusted by controlling the false discovery rate at 0.05.

closer than in the other two models. Additionally, there are some notable differences between the coupled and uncoupled simulations. The EC-Earth3P and CMCC-CM2 models have more AEWs in the coupled simulations, while the differences between the AEW track counts in the coupled and uncoupled simulations are less clear in the HadGEM3-GC3.1 model. The results from Figure 2 highlight the dominance of the southern AEW track in all three models, but also reveal that the HadGEM3-GC3.1 model has some noteworthy differences compared to the other two models.

EKE is used to examine the strength of the AEWs in the EC-Earth3P, CMCC-CM2, and HadGEM3-GC3.1 models. As in previous research, we calculate the EKE in the latitude–pressure plane using $\frac{u'^2 + v'^2}{2}$ (Bercos-Hickey et al., 2017, 2022; Hsieh & Cook, 2007), where u' and v' are the filtered zonal and meridional winds, respectively, as described in Section 2. Latitude–pressure cross-sections of EKE not only provide an indicator of AEW strength, but also allow for visualization of the north and south AEW tracks. To better understand how climate change may affect the strength of the AEWs in the three models, we compare the EKE in the historical and future simulations. Figure 3 shows the EKE, zonally-averaged between 20°W – 20°E and time-averaged for times only when waves occurred between May–November, for the coupled future minus historical simulations from the (a) EC-Earth3P, (b) CMCC-CM2, and (c) HadGEM3-GC3.1 models. The black contour lines in Figure 3 show the EKE in the historical simulations. Figure 3 shows positive anomalies in the regions of the AEW tracks for all three models, indicating larger EKE in the future simulations when compared with the historical. The EC-Earth3P (Figure 3a) and CMCC-CM2 (Figure 3b) models most clearly show a future increase in EKE in both the north and south AEW tracks, whereas the HadGEM3-GC3.1 model (Figure 3c) only shows a prominent future increase in EKE in the region of the south AEW track. A comparison of the difference (shading) and the historical (solid black lines) in Figure 3 indicates that the EKE field experiences latitudinal shifts in the future climate. In the EC-Earth3P (Figure 3a) and CMCC-CM2 (Figure 3b) models, the positive anomalies are shifted north compared to the historical field, in agreement with Bercos-Hickey and Patricola (2021), while there is a slight southern shift in the HadGEM3-GC3.1 model (Figure 3c). For the uncoupled simulations (not shown), there is also a clear future increase in EKE in the north and south AEW tracks for all three models. The results shown in Figure 3 suggest a future strengthening of the AEWs in all three models, which is in agreement with previous research (Bercos-Hickey & Patricola, 2021).

In addition to examining the effects of climate change on the EKE, we also consider the differences between the EKE in the coupled and uncoupled simulations. Figure 4 shows the EKE, zonally-averaged between 20°W – 20°E and time-averaged for times only when waves occurred between May–November, for the coupled minus uncoupled historical simulations from the (a) EC-Earth3P, (b) CMCC-CM2, and (c) HadGEM3-GC3.1 models. From Figure 4, all three models indicate less EKE in the general region of the north AEW track in the coupled

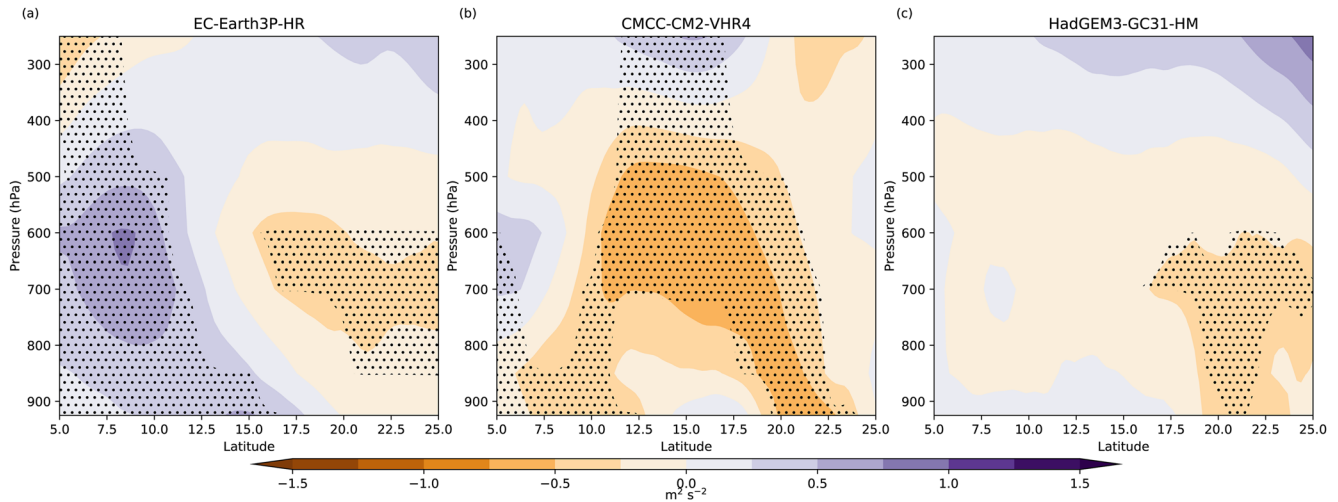


Figure 4. Eddy kinetic energy (EKE) ($\text{m}^2 \text{s}^{-2}$) zonally averaged between 20°W and 20°E from the May–November 1950–1980 average coupled minus uncoupled simulations for the (a) EC-Earth3P-HR, (b) CMCC-CM2-VHR4, and (c) HadGEM3-GC31-HM models. Time averages only include times where waves occur. Stippling refers to a significant difference in EKE between the historical coupled and uncoupled simulations using a grid-cell specific two sample t -test with the p -values adjusted by controlling the false discovery rate at 0.05.

simulations when compared with the uncoupled simulations. In the region of the south AEW track, only the CMCC-CM2 (Figure 4b) and HadGEM3-GC3.1 (Figure 4c) models indicate less EKE in the coupled simulations, whereas there is an increase in EKE in the coupled compared to the uncoupled simulations in the EC-Earth3P model (Figure 4a). The difference between the future coupled and uncoupled simulations (not shown) is similar to the historical climate, with all three models indicating less EKE in the general region of the north AEW track in the coupled simulations. One possible explanation for the difference between the coupled and uncoupled EKE is the precipitation field. There is a precipitation increase near the coast of Africa between 5 and 15°N and decrease between 15 and 25°N in the coupled simulations when compared with the uncoupled simulations. The decrease in precipitation between 15 and 25°N is likely a contributing factor to the northern track decrease in EKE in the coupled simulations, as stronger AEWs are convectively more active (Hopsch et al., 2009). It is also likely that there are differences in the large-scale circulation in the coupled versus uncoupled simulations which would in turn affect the AEJ and the energy exchange between the waves and the mean flow.

4.2. Developing and Non-Developing Waves

The EKE was used to examine the strength of the developing and non-developing AEWs. Figure 5 shows the EKE from developing minus non-developing AEWs, averaged between 20°W – 20°E and May–November, for the coupled historical and future simulations from the three models. There are positive anomalies in all panels of Figure 5 that coincide with the locations of the north and south AEW tracks. These positive anomalies clearly indicate that the EKE is larger for the developing waves than the non-developing waves in the historical and future coupled simulations of all three models. It is possible that the differences in Figure 5 are influenced by the annual cycle of EKE given that developing AEWs are more likely to occur during August and September. However, the annual cycle of EKE may also be driven by AEW activity. Although beyond the scope of this work, determining the relative contribution of the annual cycle to Figure 5 is an important area for future research. We see similar results for the uncoupled simulations (not shown), where the EKE is larger in both tracks for the developing waves than the non-developing waves in the historical and future simulations of all models. The results shown in Figure 5 suggest that AEWs that develop into TCs are stronger than their non-developing counterparts in the historical and future climates of the coupled and uncoupled simulations. These results are in agreement with previous research that found stronger developing AEWs using reanalysis data (Hopsch et al., 2009). However, here we additionally find that developing AEWs are stronger in the future climate.

The CV is used to specifically examine the strength of the AEWs along their tracks, as opposed to the EKE, which is representative of the whole region. Figure 6 shows probability density function (PDF) curves of the CV for developing and non-developing AEWs, from May–November 1950–1980 (historical) and 2020–2050

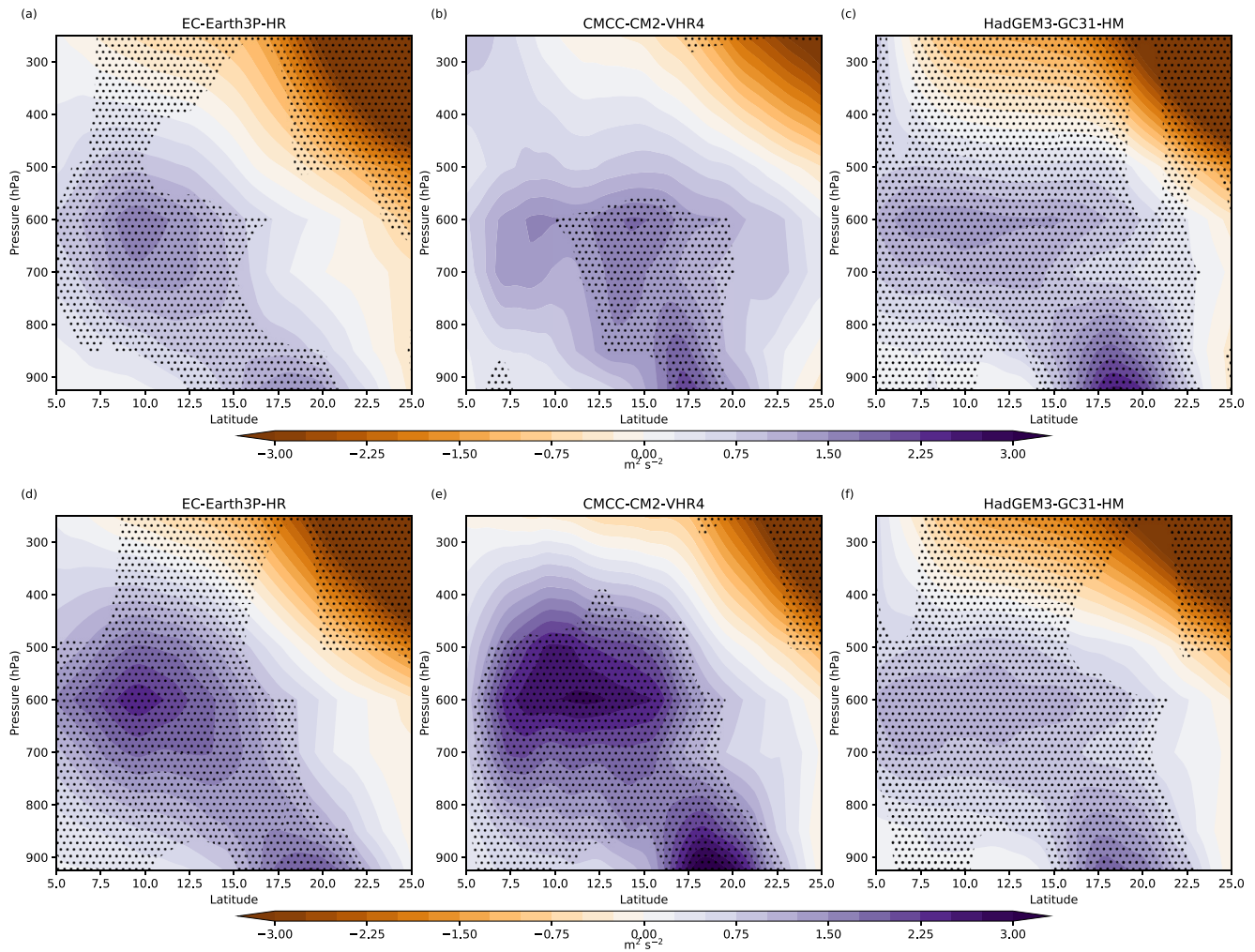


Figure 5. Eddy kinetic energy (EKE) ($\text{m}^2 \text{s}^{-2}$) from developing minus non-developing African easterly waves (AEWs), zonally averaged between 20°W and 20°E from the average coupled May–November (a–c) historical (1950–1980) and (d–f) future (2020–2050) simulations for the (a) (d) EC-Earth3P-HR, (b) (e) CMCC-CM2-VHR4, and (c) (f) HadGEM3-GC3.1-HM models. Time averages only include times where developing or non-developing waves occur. Stippling refers to a significant difference in EKE between developing and non-developing AEWs using a grid-cell specific two sample t -test with the p -values adjusted by controlling the false discovery rate at 0.05.

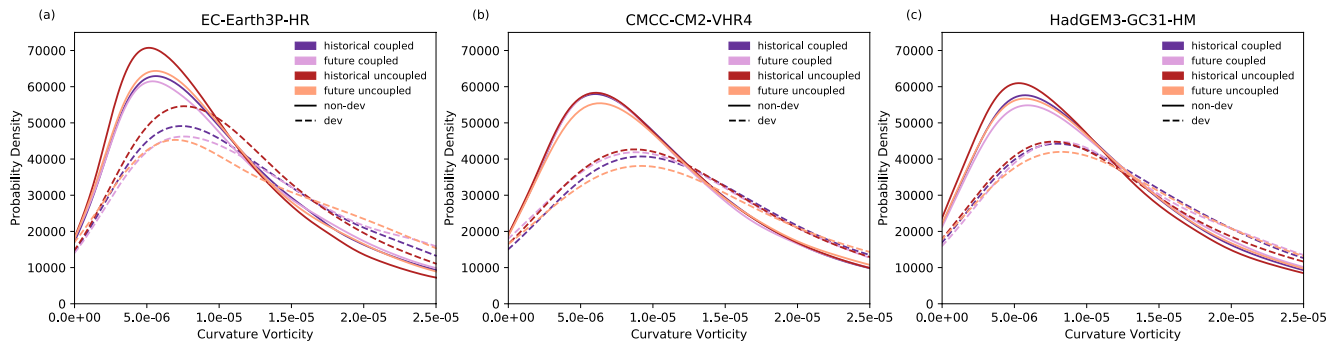


Figure 6. Probability density functions of the curvature vorticity in developing (dashed) and non-developing (solid) African easterly waves, from the May–November 1950–1980 (historical) and 2020–2050 (future) coupled and uncoupled simulations of the (a) EC-Earth3P-HR, (b) CMCC-CM2-VHR4, and (c) HadGEM3-GC3.1-HM models.

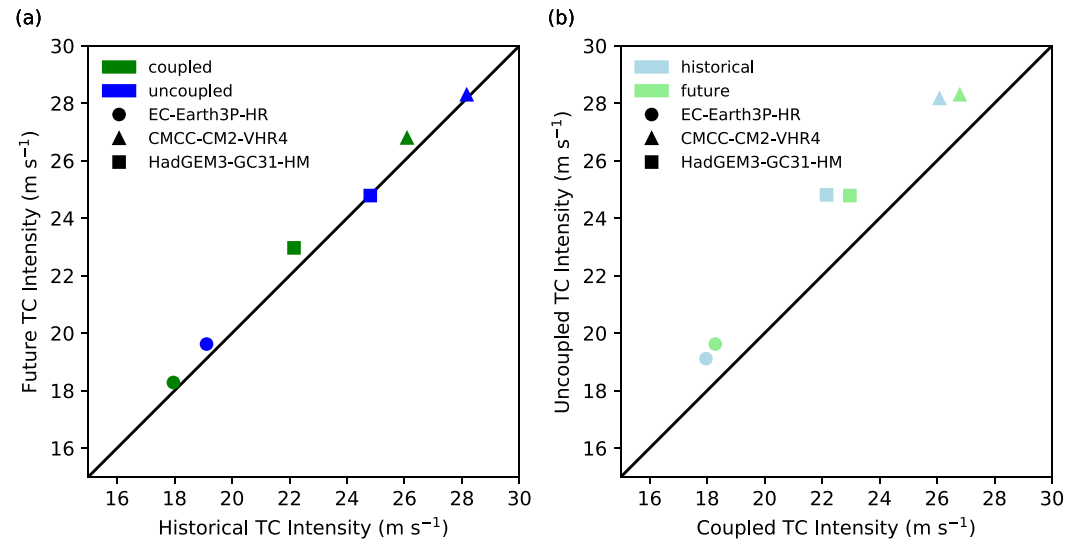


Figure 7. Scatterplot relating the intensity of tropical cyclones (TCs) in the (a) historical and future, and (b) coupled and uncoupled simulations. Intensity was calculated by averaging the lifetime maximum 10 m windspeed (m s^{-1}) of the TCs from May–November and averaged between 1950–1980 (historical) and 2020–2050 (future) for the coupled and uncoupled simulations of the three HighResMIP models.

(future) from the coupled and uncoupled simulations of the three models. There is a clear right shift of the PDF curves of the developing AEWs (Figure 6), indicating larger CV for developing waves in all simulations of the three models. Larger CV along AEW tracks is an indicator of stronger AEWs (Bercos-Hickey & Patricola, 2021; Brannan & Martin, 2019). The results therefore suggest that, based on the individual AEW tracks, developing waves are stronger than non-developing waves in the historical and future and coupled and uncoupled simulations of the three models. These results are in agreement with the EKE shown in Figure 5 and provide robust evidence that, regardless of coupled or uncoupled simulations, developing AEWs are stronger than non-developing AEWs in the historical and future climate.

5. Tropical Cyclones

In this section, we examine the May–November strength and PI of the TCs in the three HighResMIP models. We then specifically look at the differences between the TCs that do and do not develop from AEWs.

5.1. TC Characteristics

The intensity of the TCs during the May–November season is examined using the maximum 10 m windspeed over the lifetime of each TC. Figure 7 shows a scatterplot relating the (a) historical and future, and (b) coupled and uncoupled lifetime maximum 10 m windspeed of the TCs averaged from May–November and between 1950–1980 (historical) and 2020–2050 (future) for the three HighResMIP models. The solid black lines in Figure 7 represent where values on the x - and y -axes are equal. With the exception of the CMCC-CM2 and HadGEM3-GC3.1 uncoupled simulations, the remaining points in Figure 7a are above the solid black line. This indicates that TC intensity is stronger in the future climate in all of the coupled simulations as well as the uncoupled simulations for the EC-Earth3P model. For the CMCC-CM2 and HadGEM3-GC3.1 uncoupled simulations, Figure 7a indicates that there is little change in TC intensity between the historical and future climates. In contrast, all points in Figure 7b are clearly above the solid black line, indicating that TC intensity is larger in the uncoupled simulations than in the coupled simulations for all models in the historical and future climates. This result is in agreement with previous research on the effects of ocean coupling on TCs (Li & Srivier, 2018; Zarzycki, 2016). In both Figures 7a and 7b, the largest intensities occur in the CMCC-CM2 model, which is not surprising given that it has the finest resolution of the three models under consideration.

To evaluate possible factors that explain the TC intensity response to climate change, we next examined PI (Emanuel, 1986), which provides a measure of the theoretical maximum of the strength of TCs based on the thermodynamic environment that the storm moves through together with the underlying SST (Emanuel, 1986;

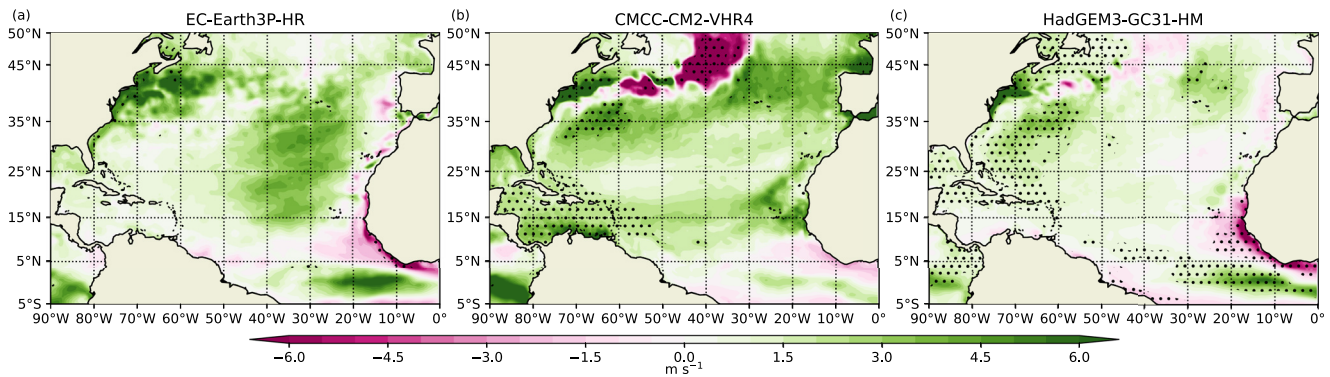


Figure 8. Potential intensity (PI) (m s^{-1}) from the coupled May–November 2020–2050 (future) average minus the 1950–1980 (historical) average for the (a) EC-Earth3P-HR, (b) CMCC-CM2-VHR4, and (c) HadGEM3-GC3.1-HM models. Time averages only include times when tropical cyclones occur. Stippling refers to a significant difference in PI between the future and historical coupled simulations using a grid-cell specific two sample *t*-test with the *p*-values adjusted by controlling the false discovery rate at 0.05.

Holland, 1997). To understand how the PI responds to future climate change, we compare the coupled historical and future simulations from the three models. Due to data availability, we were not able to examine the PI in the uncoupled simulations. Figure 8 shows the time-averaged PI (m s^{-1}) for times only when TCs occurred between May–November for the coupled future minus historical simulations from the three models. From Figure 8, we see mostly a future increase in PI during times when TCs are present in the three models. In the EC-Earth3P model (Figure 8a), there is a future increase in PI in the middle and western edge of the North Atlantic and a future decrease off of the coast of Africa, notably between 5 and 15°N. The PI in the CMCC-CM2 model (Figure 8b) experiences a future increase across the Atlantic basin, with only a slight decrease near the Gulf of Guinea. Lastly, the PI in the HadGEM3-GC3.1 model (Figure 8c) experiences a future increase in the western part of the North Atlantic and a decrease off of the coast of Africa, similar to the EC-Earth3P model. The results shown in Figure 8 can be used to interpret the TC intensity changes shown in Figure 7. Figure 7 indicates that actual TC intensity will be stronger in the future, coupled simulations. From Figure 8, the future increase in PI in large regions of the North Atlantic suggests that the future TC intensity changes in the models are driven by SST and thermodynamic factors. Additionally, analysis of the 250–850 hPa vertical wind shear (not shown) indicates regions of increased shear in the future climate, most notably in the EC-Earth3P and HadGEM3-GC3.1 models, suggesting that future TC intensity changes are less driven by the vertical wind shear.

5.2. Developed and Non-Developed Tropical Cyclones

We begin our analysis of TCs that do and do not develop from AEWs by examining their genesis locations. Figure 9 shows PDF curves of the genesis (a)–(c) latitudes and (d)–(f) longitudes of developed (dashed) and non-developed (solid) TCs in the (a) (d) EC-Earth3P-HR, (b) (e) CMCC-CM2-VHR4, and (c) (f) HadGEM3-GC3.1-HM models. In all panels of Figure 9, there is little difference in the main latitude and longitude genesis locations between the coupled and uncoupled models as well as the historical and future simulations. From Figures 9a–9c, it is clear that the dominant latitude for TC genesis in all simulations is between 10 and 15°N for developed and non-developed TCs. There is a secondary peak between 25 and 30°N that is more pronounced for the non-developed TCs. Figures 9d–9f show that the dominant longitude for TC genesis is near 70–80°W for non-developed TCs in all simulations. In contrast, the PDF curves for the developed TCs indicate TC genesis occurs near 70–80°W and 20–30°W in all simulations. The results presented in Figure 9 are perhaps not surprising, but rather they confirm what we would anticipate regarding the genesis of TCs that do and do not develop from AEWs. Non-developed TCs primarily form near the Caribbean Sea and off of the coast of Florida, whereas developed TCs primarily form in the region of the southern AEW track near the Caribbean Sea and the coast of Africa.

The intensity of the TCs that do and do not develop from AEWs is also examined using the maximum 10 m windspeed over the TC lifetime. Figure 10 shows a scatterplot relating the lifetime maximum 10 m windspeed of the TCs that do and do not develop from AEWs averaged from May–November and between 1950–1980 (historical) and 2020–2050 (future) for the coupled and uncoupled simulations of the three HighResMIP models. The solid black line in Figure 10 represents where values on the *x*- and *y*-axes are equal. From Figure 10, almost all simulations of the CMCC-CM2 and HadGEM3-GC3.1 models are below the solid black line, indicating that TC

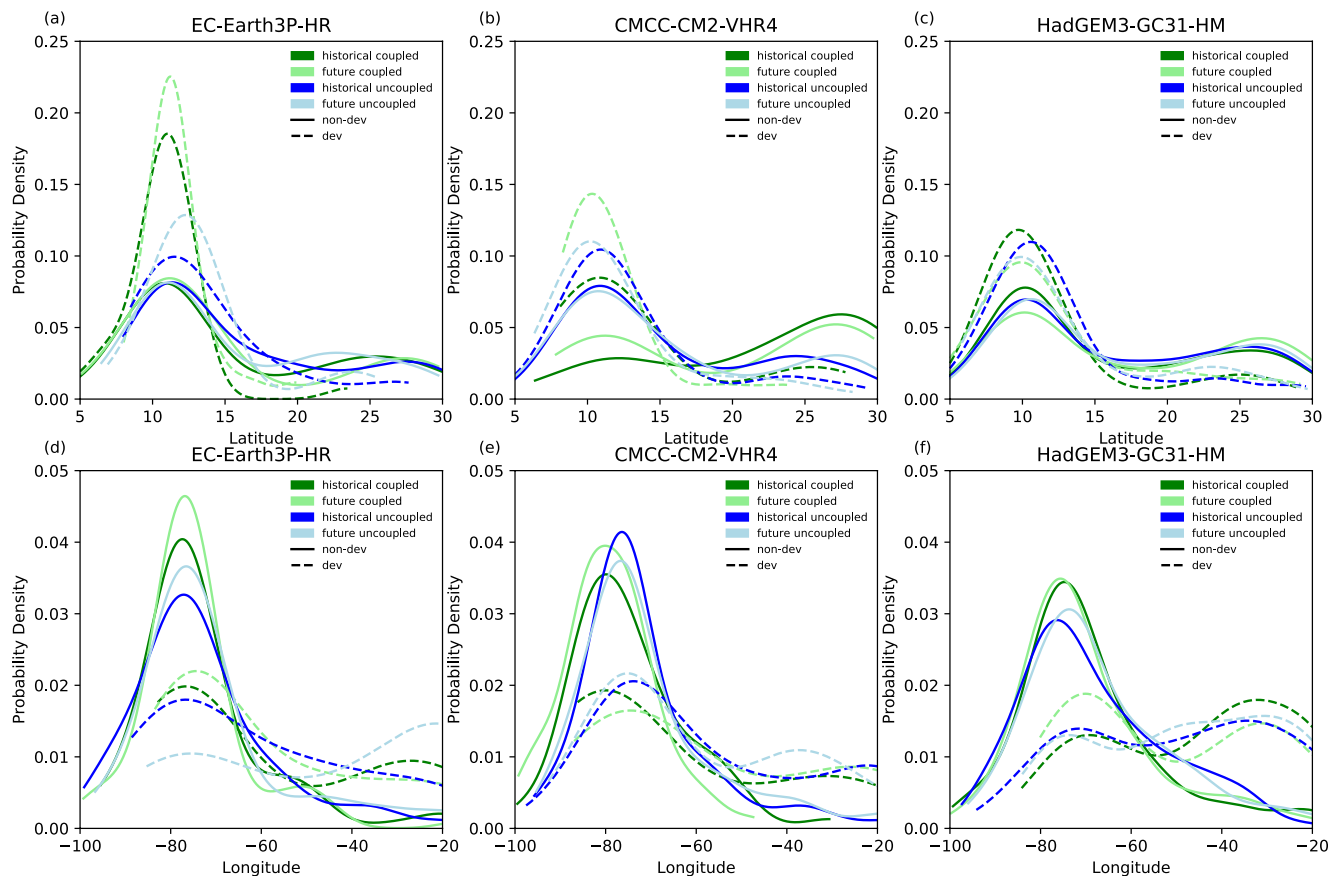


Figure 9. Probability density function curves of genesis (a–c) latitude and (d–f) longitude for tropical cyclones that developed (dashed) and did not develop (solid) from African easterly waves in the May–November historical (1950–1980) and future (2020–2050) climate of the coupled and uncoupled simulations of the (a) (d) EC-Earth3P-HR, (b) (e) CMCC-CM2-VHR4, and (c) (f) HadGEM3-GC3.1-HM models.

intensity is stronger for TCs that develop from AEWs than TCs that do not develop from AEWs. In contrast, all simulations from the EC-Earth3P model are above the black line, indicating that TC intensity is weaker for TCs that develop from AEWs. Similar to Figure 7, the largest intensity is seen in the CMCC-CM2 model in Figure 10, which is likely a function of the higher model resolution. The results presented in Figure 10 demonstrate some uncertainty in how AEWs may affect the intensity of TCs. Two of the three models suggest that TCs that develop from AEWs will be more intense in the historical and future climate, but one model contradicts this finding.

The difference in intensity between TCs that do and do not develop from AEWs is further examined using PI. Figure 11 shows the PI from TCs that developed minus TCs that did not develop from AEWs from the average coupled May–November (a)–(c) 1950–1980 and (d)–(f) 2020–2050 simulations for the (a) (d) EC-Earth3P-HR, (b) (e) CMCC-CM2-VHR4, and (c) (f) HadGEM3-GC3.1-HM models. We were not able to examine the PI in the uncoupled simulations due to data availability. Figure 11 clearly shows positive anomalies in the middle of the Atlantic basin for the historical and future simulations of the three models. Additionally, positive anomalies can be seen in all panels of Figure 11 along the coast of Africa and extending into the Atlantic Ocean near 15°N. From Figure 9, TC genesis occurs in the western Atlantic and, for developed TCs, off of the coast of Africa. The positive anomalies in Figure 11 indicate larger PI, and therefore more environmental favorability, near the regions of TC genesis for developed TCs when compared with non-developed TCs. As discussed in Section 4, it is possible that the differences in Figure 11 are influenced by the annual cycle of TCs, but determining the relative contribution of the annual cycle is beyond the scope of this work. Recall that the EKE in Figure 5 showed that developing AEWs are stronger than non-developing AEWs. Figures 5 and 11 therefore lead us to consider whether the driving force behind TC genesis from AEWs is the presence of stronger AEWs or environmental favorability, or a combination of the two factors.

The results shown in Figure 11 can be used to interpret the TC intensity changes shown in Figure 10. From Figure 10, the intensity of historical and future TCs that develop from AEWs is stronger in the CMCC-CM2

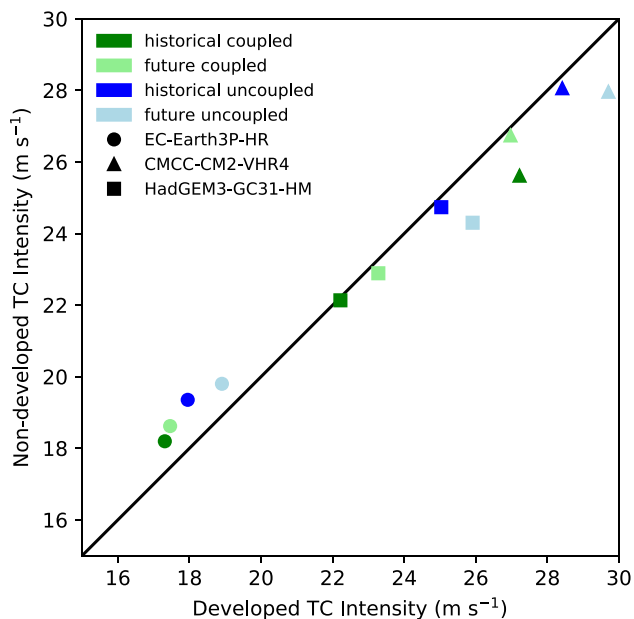


Figure 10. Scatterplot relating the intensity of tropical cyclones (TCs) that developed and TCs that did not develop from African easterly waves. Intensity was calculated by averaging the lifetime maximum 10 m windspeed (m s^{-1}) of the TCs from May–November and averaging between 1950–1980 (historical) and 2020–2050 (future) for the coupled and uncoupled simulations of the three HighResMIP models.

and HadGEM3-GC3.1 models and weaker in the EC-Earth3P model. The PI anomalies shown in Figure 11 indicate that historical and future TCs that develop from AEWs have larger PI, specifically where AEWs exit the coast of Africa, in all three of the coupled models. This suggests that the increased intensity of the TCs that develop from AEWs in the CMCC-CM2 and HadGEM3-GC3.1 models is largely driven by SST and thermodynamic factors, whereas the decreased intensity in the EC-Earth3P model may be due to additional factors, such as vertical wind shear.

6. Conclusions

Tropical cyclones can be both deadly and destructive, and it is therefore crucial to understand how TCs will respond to future climate change. African easterly waves (AEWs), which propagate westward across North Africa to the Atlantic Ocean, have been shown to serve as seedling disturbances for TCs (Avila & Pasch, 1992; Landsea, 1993). The objective of this study is to develop a better understanding of the relationship between AEWs and TCs and how this relationship may be affected by climate change. To address this objective, we examined data from the EC-Earth3P, CMCC-CM2, and HadGEM3-GC3.1 models from the HighResMIP PRIMAVERA simulations. The model simulations were run in the historical and future climate, allowing us to address the response of the AEW-TC relationship to climate change. Additionally, simulations were performed with atmosphere-ocean coupling as well as prescribed SSTs. The AEWs and TCs were tracked in the simulations using objective tracking algorithms and tracks were matched in time and space to determine AEWs that develop into TCs. Our main findings are as follows: Future changes in AEW frequency are not a clear indicator of

future changes in TC frequency. Developing AEWs are stronger than non-developing AEWs in the historical and future climates, and therefore strong AEWs may suggest future TC development. TCs that develop from AEWs, however, have more favorable environmental conditions directly off of the coast of Africa and in the Atlantic basin in the historical and future climates, providing ideal conditions for cyclogenesis.

We found large disagreement among the three models on the future change in frequency of AEWs and TCs in the North Atlantic. Additionally, the effects of atmosphere-ocean coupling on AEW and TC frequency are not consistent across the three models. The model disagreement indicates that there is still uncertainty in how climate change will affect the seasonal number of AEWs and TCs. We also found that the signs of the future change of AEW and TC frequency (i.e., future increase or decrease) are not always in agreement. By specifically examining developing and non-developing AEWs, we found that even if the total number of AEWs increases in the future climate, the percent of developing AEWs can decrease. These results suggest that future changes in AEW frequency may not necessarily correspond to future changes in TC frequency, and that AEW frequency is not a limiting factor for future tropical cyclogenesis.

In contrast, there was better model agreement regarding the strength of the AEWs. All three models showed a future increase in EKE in the regions of the north and south AEW tracks, indicating stronger future AEWs which is consistent with Bercos-Hickey and Patricola (2021). However, the effects of atmosphere-ocean coupling versus prescribed SSTs on the EKE indicated weaker AEWs in the north AEW track in the coupled simulations, possibly due to a decrease in precipitation. There was strong agreement between the models when we compared the EKE of developing and non-developing AEWs. Developing AEWs had larger EKE than non-developing AEWs in the regions of the north and south AEW tracks in the historical and future simulations of the three models. We also examined the CV of the individual AEW tracks and found, consistent with the EKE analysis, that the CV is larger for developing AEWs in all simulations of the three models. These results indicate that developing AEWs are stronger than non-developing AEWs, which is in agreement with previous research that looked at historical reanalysis data (Hopsch et al., 2009). In this study, however, we not only see stronger developing AEWs in the historical climate, but we also found stronger developing AEWs in the future climate, regardless of atmosphere-ocean coupling or prescribed SSTs.

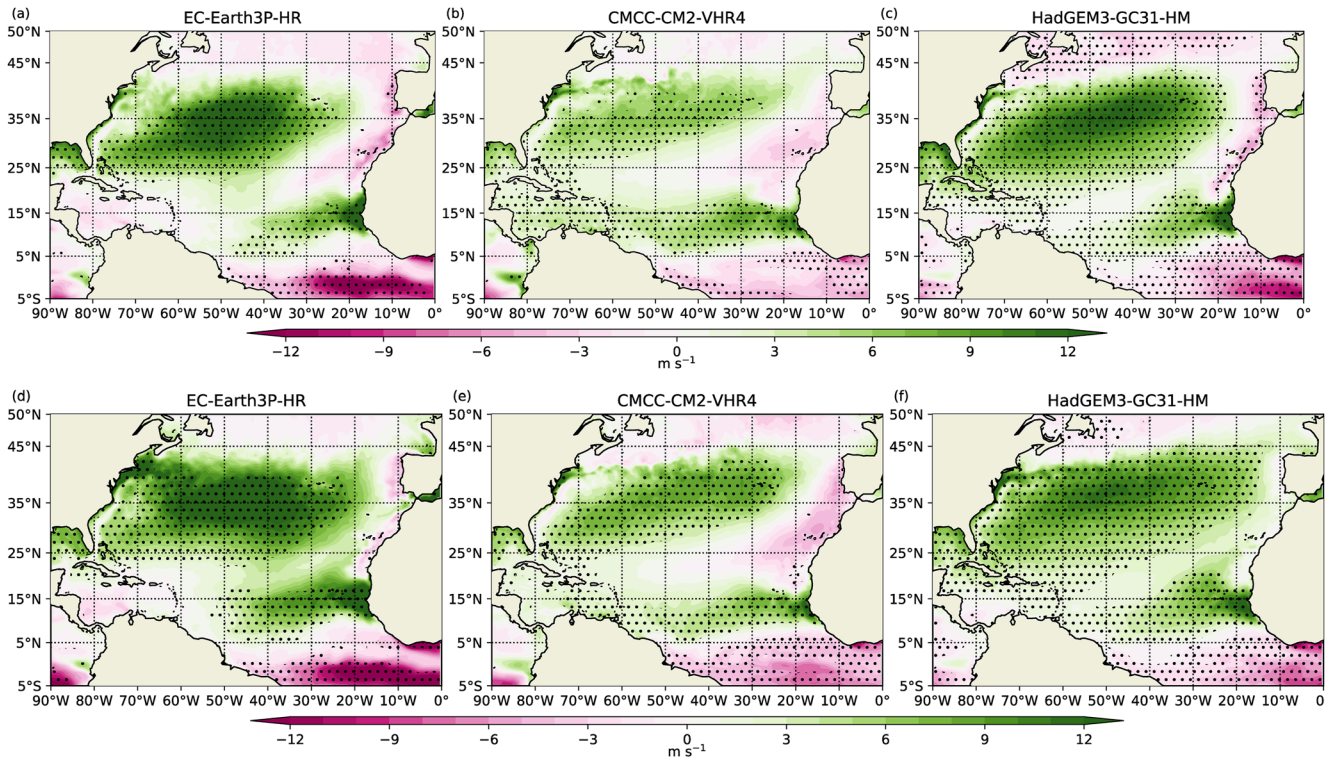


Figure 11. Potential intensity (PI) (m s^{-1}) from tropical cyclones (TCs) that developed minus TCs that did not develop from African easterly waves (AEWs) from the average coupled May–November (a–c) 1950–1980 and (d–f) 2020–2050 simulations for the (a) (d) EC-Earth3P-HR, (b) (e) CMCC-CM2-VHR4, and (c) (f) HadGEM3-GC3.1-HM models. Time averages only include times where TCs that develop or do not develop from AEWs occur. Stippling refers to a significant difference in PI between TC that developed and TCs that did not develop from AEWs using a grid-cell specific two sample *t*-test with the *p*-values adjusted by controlling the false discovery rate at 0.05.

With respect to the TCs, we found a slight future increase in TC intensity (based on maximum 10 m windspeed over the TC lifetime) for all models. Future increases in PI in all models suggest that the future increase in TC intensity is largely driven by SST and thermodynamic factors. It is also possible that there is a stochastic component in TC intensity that may not be captured by environmental factors. Additionally, there is a clear increase in TC intensity in the uncoupled simulations when compared with the atmosphere–ocean coupled simulations. When looking specifically at TCs that do and do not develop from AEWs, we found that TCs that develop from AEWs are more intense in two of the three models. Comparison of the PI from TCs that do and do not develop from AEWs shows good agreement across the three models. For the TCs that develop from AEWs, the PI is larger in the middle of the North Atlantic and off of the coast of Africa near 15°N in the historical and future climates. This suggests that, in two of the three models, the increase in intensity for TCs that develop from AEWs is likely driven by SST and thermodynamic factors. Additionally, the regions of larger PI, and therefore increased environmental favorability, for developed TCs coincide with the regions of TC genesis off of the coast of Africa. These results bring into consideration whether the driving force behind TC genesis from AEWs is the presence of stronger AEWs or the favorable environment that these waves enter into, or a combination of the two factors.

Our results show that AEW frequency is not a good indicator of TC activity, but that AEW strength as well as environmental conditions conducive to strong TCs are good indicators of AEWs that develop into TCs in the historical and future climates. The results presented in this study are, of course, limited by the datasets. Here we examined three models from the HighResMIP PRIMAVERA simulations. Analysis of additional models outside of the HighResMIP PRIMAVERA simulations, particularly high-resolution models, would contribute to the robustness of the results. As noted by Roberts et al. (2020a), the models used in this study produced a lower frequency of North Atlantic TCs, which limits the sample size of TCs that develop from AEWs. Additional research with a larger sample size of TCs is needed to further establish the characteristics of the AEW-TC relationship and how this relationship may respond to future climate change. The results in this study, however, indicate the importance of examining both the AEWs and the environment when assessing how future climate change will affect the AEW-TC relationship.

Data Availability Statement

The HighResMIP-PRIMAVERA climate model outputs are available on the Earth System Grid Federation nodes (<https://esgf-index1.ceda.ac.uk/search/cmip6-ceda>). The model data can also be accessed at the UK Centre for Environmental Data Analysis's JASMIN platform (<https://www.ceda.ac.uk/services/jasmin/>). The AEW tracking code is located on Zenodo (<https://zenodo.org/badge/latestdoi/290061935>) and the TC tracks can be accessed through the UK Centre for Environmental Data Analysis under reference Roberts (2019).

Acknowledgments

The authors thank Fabrice Chauvin and two additional reviewers for their constructive and insightful comments. This material is based upon work supported by the U.S. Department of Energy, Office of Science, Office of Biological and Environmental Research, Climate and Environmental Sciences Division, Regional & Global Model Analysis Program, under Award Number DE-AC02-05CH11231. C.M.P. acknowledges support from the U.S. Department of Energy, Office of Science, Office of Biological and Environmental Research, Earth and Environmental Systems Modeling (EESM) Program, Early Career Research Program Award Number DE-SC0021109. This research used resources of the National Energy Research Scientific Computing Center (NERSC), a U.S. Department of Energy Office of Science User Facility operated under Contract No. DE-AC02-05CH11231. The authors thank the modeling groups within PRIMAVERA (a European Union Horizon 2020 project under Grant Agreement 641727) for producing the multi-model simulations and providing the climate model outputs via the Earth System Grid Federation (ESGF). The authors greatly appreciate Malcolm Roberts and Jon Seddon (UK Met Office Hadley Centre) for their help in accessing the model data through the UK Centre for Environmental Data Analysis's JASMIN platform.

References

- Agudelo, P. A., Hoyos, C. D., Curry, J. A., & Webster, P. J. (2011). Probabilistic discrimination between large-scale environments of intensifying and decaying African Easterly Waves. *Climate Dynamics*, *36*(7–8), 1379–1401. <https://doi.org/10.1007/s00382-010-0851-x>
- Avila, L. A. (1991). Atlantic tropical systems of 1990. *Monthly Weather Review*, *119*(8), 2027–2033. [https://doi.org/10.1175/1520-0493\(1991\)119<2027:ATSO>2.0.CO;2](https://doi.org/10.1175/1520-0493(1991)119<2027:ATSO>2.0.CO;2)
- Avila, L. A., & Pasch, R. J. (1992). Atlantic tropical systems of 1991. *Monthly Weather Review*, *120*(11), 2688–2696. [https://doi.org/10.1175/1520-0493\(1992\)120<2688:ATSO>2.0.CO;2](https://doi.org/10.1175/1520-0493(1992)120<2688:ATSO>2.0.CO;2)
- Bain, C. L., Williams, K. D., Milton, S. F., & Heming, J. T. (2014). Objective tracking of African easterly waves in Met Office models. *Quarterly Journal of the Royal Meteorological Society*, *140*(678), 47–57. <https://doi.org/10.1002/qj.2110>
- Bender, M. A., Knutson, T. R., Tuleya, R. E., Sirutis, J. J., Vecchi, G. A., Garner, S. T., & Held, I. M. (2010). Modeled impact of anthropogenic warming on the frequency of intense Atlantic Hurricanes. *Science*, *327*(5964), 454–458. <https://doi.org/10.1126/science.1180568>
- Bercos-Hickey, E., Nathan, T. R., & Chen, S.-H. (2017). Saharan dust and the African easterly jet-African easterly wave system: Structure, location, and energetics. *Quarterly Journal of the Royal Meteorological Society*, *143*(708), 2797–2808. <https://doi.org/10.1002/qj.3128>
- Bercos-Hickey, E., Nathan, T. R., & Chen, S.-H. (2022). Effects of Saharan dust Aerosols and West African precipitation on the energetics of African easterly waves. *Journal of the Atmospheric Sciences*, *79*, 1911–1926. <https://doi.org/10.1175/JAS-D-21-0157.1>
- Bercos-Hickey, E., & Patricola, C. M. (2021). Anthropogenic influences on the African easterly jet–African easterly wave system. *Climate Dynamics*, *57*(9–10), 2779–2792. <https://doi.org/10.1007/s00382-021-05838-1>
- Berry, G. J., Thorncroft, C. D., & Hewson, T. (2007). African easterly waves during 2004—Analysis using objective techniques. *Monthly Weather Review*, *135*(4), 1251–1267. <https://doi.org/10.1175/MWR3343.1>
- Bhatia, K., Vecchi, G., Murakami, H., Underwood, S., & Kossin, J. (2018). Projected response of tropical cyclone intensity and intensification in a global climate model. *Journal of Climate*, *31*(20), 8281–8303. <https://doi.org/10.1175/JCLI-D-17-0898.1>
- Bourdin, S., Fromang, S., Dulac, W., Cattiaux, J., & Chauvin, F. (2022). Intercomparison of four algorithms for detecting tropical cyclones using ERA5. *Geoscientific Model Development*, *15*(17), 6759–6786. <https://doi.org/10.5194/gmd-15-6759-2022>
- Brammer, A., & Thorncroft, C. D. (2015). Variability and evolution of African easterly wave structures and their relationship with tropical cyclogenesis over the eastern Atlantic. *Monthly Weather Review*, *143*(12), 4975–4995. <https://doi.org/10.1175/MWR-D-15-0106.1>
- Brammer, A., & Thorncroft, C. D. (2017). Spatial and temporal variability of the three-dimensional flow around African easterly waves. *Monthly Weather Review*, *145*(7), 2879–2895. <https://doi.org/10.1175/MWR-D-16-0454.1>
- Brannan, A. L., & Martin, E. R. (2019). Future characteristics of African easterly wave tracks. *Climate Dynamics*, *52*(9–10), 5567–5584. <https://doi.org/10.1007/s00382-018-4465-z>
- Burpee, R. W. (1972). The origin and structure of easterly waves in the lower troposphere of North Africa. *Journal of the Atmospheric Sciences*, *29*(1), 77–90. [https://doi.org/10.1175/1520-0469\(1972\)029<0077:TOASOE>2.0.CO;2](https://doi.org/10.1175/1520-0469(1972)029<0077:TOASOE>2.0.CO;2)
- Camargo, S. J. (2013). Global and regional aspects of tropical cyclone activity in the CMIP5 models. *Journal of Climate*, *26*(24), 9880–9902. <https://doi.org/10.1175/JCLI-D-12-00549.1>
- Caron, L.-P., & Jones, C. G. (2012). Understanding and simulating the link between African easterly waves and Atlantic tropical cyclones using a regional climate model: The role of domain size and lateral boundary conditions. *Climate Dynamics*, *39*(1–2), 113–135. <https://doi.org/10.1007/s00382-011-1160-8>
- Cervený, R. S., Bessemoulin, P., Burt, C. C., Cooper, M. A., Cunjje, Z., Dewan, A., et al. (2017). WMO assessment of weather and climate mortality extremes: Lightning, tropical cyclones, tornadoes, and hail. *Weather, Climate, and Society*, *9*(3), 487–497. <https://doi.org/10.1175/WCAS-D-16-0120.1>
- Chauvin, F., Pilon, R., Palany, P., & Belmadani, A. (2020). Future changes in Atlantic hurricanes with the rotated-stretched ARPEGE-Climat at very high resolution. *Climate Dynamics*, *54*(1–2), 947–972. <https://doi.org/10.1007/s00382-019-05040-4>
- Cherchi, A., Fogli, P. G., Lovato, T., Peano, D., Iovino, D., Gualdi, S., et al. (2019). Global mean climate and main patterns of variability in the CMCC-CM2 coupled model. *Journal of Advances in Modeling Earth Systems*, *11*, 185–209. <https://doi.org/10.1029/2018MS001369>
- Danso, D. K., Patricola, C. M., & Bercos-Hickey, E. (2022). Influence of African easterly wave suppression on Atlantic tropical cyclone activity in a convection-permitting model. *Geophysical Research Letters*, *49*(22), e2022GL100590. <https://doi.org/10.1029/2022GL100590>
- Davis, C. A. (2018). Resolving tropical cyclone intensity in models. *Geophysical Research Letters*, *45*(4), 2082–2087. <https://doi.org/10.1002/2017GL076966>
- Dunkerton, T. J., Montgomery, M. T., & Wang, Z. (2009). Tropical cyclogenesis in a tropical wave critical layer: Easterly waves. *Atmospheric Chemistry and Physics*, *9*(15), 5587–5646. <https://doi.org/10.5194/acp-9-5587-2009>
- Emanuel, K. (2022). Tropical cyclone seeds, transition probabilities, and Genesis. *Journal of Climate*, *35*(11), 3557–3566. <https://doi.org/10.1175/JCLI-D-21-0922.1>
- Emanuel, K. A. (1986). An air-sea interaction theory for tropical cyclones. Part I: Steady-state maintenance. *Journal of the Atmospheric Sciences*, *43*(6), 585–605. [https://doi.org/10.1175/1520-0469\(1986\)043<0585:AASITF>2.0.CO;2](https://doi.org/10.1175/1520-0469(1986)043<0585:AASITF>2.0.CO;2)
- Emanuel, K. A. (1987). The dependence of hurricane intensity on climate. *Nature*, *326*(6112), 483–485. <https://doi.org/10.1038/326483a0>
- Emanuel, K. A. (1988). The maximum intensity of hurricanes. *Journal of the Atmospheric Sciences*, *45*(7), 1143–1155. [https://doi.org/10.1175/1520-0469\(1988\)045<1143:TMIH>2.0.CO;2](https://doi.org/10.1175/1520-0469(1988)045<1143:TMIH>2.0.CO;2)
- Emanuel, K. A. (2013). Downscaling CMIP5 climate models shows increased tropical cyclone activity over the 21st century. *Proceedings of the National Academy of Sciences of the United States of America*, *110*(30), 12219–12224. <https://doi.org/10.1073/pnas.1301293110>
- Fink, A. H., & Reiner, A. (2003). Spatiotemporal variability of the relation between African easterly waves and west African Squall lines in 1998 and 1999. *Journal of Geophysical Research*, *108*(D11), 4332. <https://doi.org/10.1029/2002JD002816>

- Frank, N. L. (1970). Atlantic tropical systems of 1969. *Monthly Weather Review*, 98(4), 307–314. [https://doi.org/10.1175/1520-0493\(1970\)098<0307:ATSO>2.3.CO;2](https://doi.org/10.1175/1520-0493(1970)098<0307:ATSO>2.3.CO;2)
- Frank, W. M., & Ritchie, E. A. (2001). Effects of vertical wind shear on the intensity and structure of numerically simulated hurricanes. *Monthly Weather Review*, 129(9), 2249–2269. [https://doi.org/10.1175/1520-0493\(2001\)129<2249:EOVWSO>2.0.CO;2](https://doi.org/10.1175/1520-0493(2001)129<2249:EOVWSO>2.0.CO;2)
- Garner, A. J., Mann, M. E., Emanuel, K. A., Kopp, R. E., Lin, N., Alley, R. B., et al. (2017). Impact of climate change on New York City's coastal flood hazard: Increasing flood heights from the preindustrial to 2300 CE. *Proceedings of the National Academy of Sciences of the United States of America*, 114(45), 11861–11866. <https://doi.org/10.1073/pnas.1703568114>
- Gray, W. M. (1968). Global view of the origin of tropical disturbances and storms. *Monthly Weather Review*, 96(10), 669–700. [https://doi.org/10.1175/1520-0493\(1968\)096<0669:GVOTOO>2.0.CO;2](https://doi.org/10.1175/1520-0493(1968)096<0669:GVOTOO>2.0.CO;2)
- Grossmann, I., & Morgan, M. G. (2011). Tropical cyclones, climate change, and scientific uncertainty: What do we know, what does it mean, and what should be done? *Climate Change*, 108(3), 543–579. <https://doi.org/10.1007/s10584-011-0020-1>
- Gualdi, S., Scoccimarro, E., & Navarra, A. (2008). Changes in tropical cyclone activity due to global warming: Results from a high-resolution coupled general circulation model. *Journal of Climate*, 21(20), 5204–5228. <https://doi.org/10.1175/2008JCLI1921.1>
- Haarsma, R., Acosta, M., Bakhshi, R., Bretonnière, P. A., Caron, L. P., Castrillo, M., et al. (2020). HighResMIP versions of EC-Earth: EC-Earth3P and EC-Earth3P-HR – Description, model computational performance and basic validation. *Geoscientific Model Development*, 13(8), 3507–3527. <https://doi.org/10.5194/gmd-13-3507-2020>
- Haarsma, R. J., Roberts, M. J., Vidale, P. L., Senior, C. A., Bellucci, A., Bao, Q., et al. (2016). High resolution model Intercomparison project (HighResMIP v1.0) for CMIP6. *Geoscientific Model Development*, 9(11), 4185–4208. <https://doi.org/10.5194/gmd-9-4185-2016>
- Hannah, W. M., & Aiyyer, A. (2017). Reduced African easterly wave activity with quadrupled CO₂ in the Superparameterized CESM. *Journal of Climate*, 30(20), 8253–8274. <https://doi.org/10.1175/JCLI-D-16-0822.1>
- Hill, K. A., & Lackmann, G. M. (2011). The impact of future climate change on TC intensity and structure: A downscaling approach. *Journal of Climate*, 24(17), 4644–4661. <https://doi.org/10.1175/2011JCLI3761.1>
- Hodges, K., Cobb, A., & Vidale, P. L. (2017). How well are tropical cyclones represented in reanalysis datasets? *Journal of Climate*, 30(14), 5243–5264. <https://doi.org/10.1175/JCLI-D-16-0557.1>
- Holland, G., & Bruyère, C. L. (2014). Recent intense hurricane response to global climate change. *Climate Dynamics*, 42(3–4), 617–627. <https://doi.org/10.1007/s00382-013-1713-0>
- Holland, G. J. (1997). The maximum potential intensity of tropical cyclones. *Journal of the Atmospheric Sciences*, 54(21), 2519–2541. [https://doi.org/10.1175/1520-0469\(1997\)054<2519:TMPIOT>2.0.CO;2](https://doi.org/10.1175/1520-0469(1997)054<2519:TMPIOT>2.0.CO;2)
- Hoogewind, K. A., Chavas, D. R., Schenkel, B. A., & O'Neill, M. E. (2020). Exploring controls on tropical cyclone count through the geography of environmental favorability. *Journal of Climate*, 33(5), 1725–1745. <https://doi.org/10.1175/JCLI-D-18-0862.1>
- Hopsch, S. B., Thorncroft, C. D., Hodges, K., & Aiyyer, A. (2007). West African storm tracks and their relationship to Atlantic tropical cyclones. *Journal of Climate*, 20(11), 2468–2483. <https://doi.org/10.1175/JCLI4139.1>
- Hopsch, S. B., Thorncroft, C. D., & Tyle, K. R. (2009). Analysis of African easterly wave structures and their role in influencing tropical cyclogenesis. *Monthly Weather Review*, 138(4), 1399–1419. <https://doi.org/10.1175/2009MWR2760.1>
- Horn, M., Walsh, K., Zhao, M., Camargo, S. J., Scoccimarro, E., Murakami, H., et al. (2014). Tracking Scheme dependence of simulated tropical cyclone response to idealized climate simulations. *Journal of Climate*, 27(24), 9197–9213. <https://doi.org/10.1175/JCLI-D-14-00200.1>
- Hsieh, J.-S., & Cook, K. H. (2007). A study of the energetics of African easterly waves using a regional climate Model. *Journal of the Atmospheric Sciences*, 64(2), 421–440. <https://doi.org/10.1175/JAS3851.1>
- Hsieh, T., Yang, W., Vecchi, G. A., & Zhao, M. (2022). Model spread in the tropical cyclone frequency and seed propensity index across global warming and ENSO-like perturbations. *Geophysical Research Letters*, 49(7), e2021GL097157. <https://doi.org/10.1029/2021gl097157>
- Hsieh, T.-L., Vecchi, G. A., Yang, W., Held, I. M., & Garner, S. T. (2020). Large-scale control on the frequency of tropical cyclones and seeds: A consistent relationship across a hierarchy of global atmospheric models. *Climate Dynamics*, 55(11–12), 3177–3196. <https://doi.org/10.1007/s00382-020-05446-5>
- Kebe, I., Diallo, I., Sylla, M. B., De Sales, F., & Diedhiou, A. (2020). Late 21st century projected changes in the relationship between precipitation, African easterly jet, and African easterly waves. *Atmosphere*, 11(4), 353. <https://doi.org/10.3390/atmos11040353>
- Kennedy, J., Reyner, N., Millington, S. C., & Saunby, M. (2017). The Met Office Hadley Centre sea ice and sea-surface temperature data set, version 2, part 2: Sea surface temperature analysis.
- Knutson, T., Camargo, S. J., Chan, J. C. L., Emanuel, K., Ho, C. H., Kossin, J., et al. (2020). Tropical cyclones and climate change assessment: Part II: Projected response to anthropogenic warming. *Bulletin of the American Meteorological Society*, 101(3), E303–E322. <https://doi.org/10.1175/BAMS-D-18-0194.1>
- Knutson, T. R., McBride, J. L., Chan, J., Emanuel, K., Holland, G., Landsea, C., et al. (2010). Tropical cyclones and climate change. *Nature Geoscience*, 3, 157–163. <https://doi.org/10.1038/ngeo779>
- Knutson, T. R., Sirutis, J. J., Garner, S. T., Vecchi, G. A., & Held, I. M. (2008). Simulated reduction in Atlantic hurricane frequency under twenty-first-century warming conditions. *Nature Geoscience*, 1(6), 359–364. <https://doi.org/10.1038/ngeo202>
- Knutson, T. R., & Tuleya, R. E. (2004). Impact of CO₂-induced warming on simulated hurricane intensity and precipitation: Sensitivity to the choice of climate model and convective parameterization. *Journal of Climate*, 17(18), 3477–3495. [https://doi.org/10.1175/1520-0442\(2004\)017<3477:IOCWOS>2.0.CO;2](https://doi.org/10.1175/1520-0442(2004)017<3477:IOCWOS>2.0.CO;2)
- Landsea, C. (2007). Counting Atlantic tropical cyclones back to 1900. *Eos Transactions American Geophysical Union*, 88(18), 197–202. <https://doi.org/10.1029/2007EO180001>
- Landsea, C. W. (1993). A climatology of intense (or major) Atlantic hurricanes. *Monthly Weather Review*, 121(6), 1703–1713. [https://doi.org/10.1175/1520-0493\(1993\)121<1703:ACOIMA>2.0.CO;2](https://doi.org/10.1175/1520-0493(1993)121<1703:ACOIMA>2.0.CO;2)
- Li, H., & Srivler, R. L. (2018). Tropical cyclone activity in the high-resolution community Earth system model and the impact of ocean coupling. *Journal of Advances in Modeling Earth Systems*, 10(1), 165–186. <https://doi.org/10.1002/2017MS001199>
- Little, C. M., Horton, R. M., Kopp, R. E., Oppenheimer, M., Vecchi, G. A., & Villarini, G. (2015). Joint projections of US East Coast sea level and storm surge. *Nature Climate Change*, 5(12), 1114–1120. <https://doi.org/10.1038/nclimate2801>
- Loring, B., O'Brien, T. A., Elbasha, A. E., Johnson, J. N., Krishnan, H., Keen, N., & Prabhat (2016). *The CASCADE SFA: Toolkit for extreme climate analysis*. Lawrence Berkeley National Lab. <https://doi.org/10.20358/C8C651>
- Manganello, J. V., Hodges, K. I., Kinter, J. L., Cash, B. A., Marx, L., Jung, T., et al. (2012). Tropical cyclone climatology in a 10-km global atmospheric GCM: Toward weather-resolving climate modeling. *Journal of Climate*, 25(11), 3867–3893. <https://doi.org/10.1175/JCLI-D-11-00346.1>
- Martin, E. R., & Thorncroft, C. (2015). Representation of African easterly waves in CMIP5 models. *Journal of Climate*, 28(19), 7702–7715. <https://doi.org/10.1175/JCLI-D-15-0145.1>

- Meinshausen, M., Smith, S. J., Calvin, K., Daniel, J. S., Kainuma, M. L. T., Lamarque, J. F., et al. (2011). The RCP greenhouse gas concentrations and their extensions from 1765 to 2300. *Climate Change*, *109*(1–2), 213–241. <https://doi.org/10.1007/s10584-011-0156-z>
- Mendelsohn, R., Emanuel, K., Chonabayashi, S., & Bakkensen, L. (2012). The impact of climate change on global tropical cyclone damage. *Nature Climate Change*, *2*(3), 205–209. <https://doi.org/10.1038/nclimate1357>
- NOAA. (2021). U.S. Billion-dollar weather and climate disasters. <https://doi.org/10.25921/stkw-7w73>
- Patricola, C. M., Saravanan, R., & Chang, P. (2018). The response of Atlantic tropical cyclones to suppression of African easterly waves. *Geophysical Research Letters*, *45*(1), 471–479. <https://doi.org/10.1002/2017GL076081>
- Patricola, C. M., & Wehner, M. F. (2018). Anthropogenic influences on major tropical cyclone events. *Nature*, *563*(7731), 339–346. <https://doi.org/10.1038/s41586-018-0673-2>
- Pytharoulis, I., & Thorncroft, C. D. (1999). The low-level structure of African easterly waves in 1995. *Monthly Weather Review*, *127*(10), 2266–2280. [https://doi.org/10.1175/1520-0493\(1999\)127<2266:TLLSOA>2.0.CO;2](https://doi.org/10.1175/1520-0493(1999)127<2266:TLLSOA>2.0.CO;2)
- Risser, M. D., & Wehner, M. F. (2017). Attributable human-induced changes in the likelihood and magnitude of the observed extreme precipitation during hurricane Harvey. *Geophysical Research Letters*, *44*(24), 12457–12464. <https://doi.org/10.1002/2017GL075888>
- Roberts, M. (2019). CMIP6 HighResMIP: Tropical storm tracks as calculated by the TRACK algorithm. Retrieved from <https://catalogue.ceda.ac.uk/uuid/0b42715a7a804290afa9b7e31f5d7753>
- Roberts, M. J., Baker, A., Blockley, E. W., Calvert, D., Coward, A., Hewitt, H. T., et al. (2019). Description of the resolution hierarchy of the global coupled HadGEM3-GC3.1 model as used in CMIP6 HighResMIP experiments. *Geoscientific Model Development*, *12*, 4999–5028. <https://doi.org/10.5194/gmd-12-4999-2019>
- Roberts, M. J., Camp, J., Seddon, J., Vidale, P. L., Hodges, K., Vanniere, B., et al. (2020a). Impact of model resolution on tropical cyclone simulation using the HighResMIP-PRIMAVERA multimodel ensemble. *Journal of Climate*, *33*(7), 2557–2583. <https://doi.org/10.1175/JCLI-D-19-0639.1>
- Roberts, M. J., Camp, J., Seddon, J., Vidale, P. L., Hodges, K., Vanniere, B., et al. (2020b). Projected future changes in tropical cyclones using the CMIP6 HighResMIP multimodel ensemble. *Geophysical Research Letters*, *47*, e2020GL088662. <https://doi.org/10.1029/2020GL088662>
- Russell, J. O., Aiyyer, A., White, J. D., & Hannah, W. (2017). Revisiting the connection between African easterly waves and Atlantic tropical cyclogenesis. *Geophysical Research Letters*, *44*(1), 587–595. <https://doi.org/10.1002/2016GL071236>
- Satoh, M., Nihonmatsu, R., & Kubokawa, H. (2013). Environmental conditions for tropical cyclogenesis associated with African easterly waves. *SOLA*, *9*(0), 120–124. <https://doi.org/10.2151/sola.2013-027>
- Scoccimarro, E., Gualdi, S., Villarini, G., Vecchi, G. A., Zhao, M., Walsh, K., & Navarra, A. (2014). Intense precipitation events associated with landfalling tropical cyclones in response to a warmer climate and increased CO₂. *Journal of Climate*, *27*(12), 4642–4654. <https://doi.org/10.1175/JCLI-D-14-00065.1>
- Skinner, C. B., & Diffenbaugh, N. S. (2014). Projected changes in African easterly wave intensity and track in response to greenhouse forcing. *Proceedings of the National Academy of Sciences of the United States of America*, *111*(19), 6882–6887. <https://doi.org/10.1073/pnas.1319597111>
- Sobel, A. H., Camargo, S. J., Hall, T. M., Lee, C.-Y., Tippett, M. K., & Wing, A. A. (2016). Human influence on tropical cyclone intensity. *Science*, *353*(6296), 242–246. <https://doi.org/10.1126/science.aaf6574>
- Sobel, A. H., Wing, A. A., Camargo, S. J., Patricola, C. M., Vecchi, G. A., Lee, C., & Tippett, M. K. (2021). Tropical cyclone frequency. *Earth's Future*, *9*(12), e2021EF002275. <https://doi.org/10.1029/2021EF002275>
- Sugi, M., Yamada, Y., Yoshida, K., Mizuta, R., Nakano, M., Kodama, C., & Satoh, M. (2020). Future changes in the global frequency of tropical cyclone seeds. *SOLA*, *16*(0), 70–74. <https://doi.org/10.2151/sola.2020-012>
- Thorncroft, C. D., & Hodges, K. (2001). African easterly wave variability and its relationship to Atlantic tropical cyclone activity. *Journal of Climate*, *14*(6), 1166–1179. [https://doi.org/10.1175/1520-0442\(2001\)014<1166:AEWVAI>2.0.CO;2](https://doi.org/10.1175/1520-0442(2001)014<1166:AEWVAI>2.0.CO;2)
- Tory, K. J., Chand, S. S., McBride, J. L., Ye, H., & Dare, R. A. (2013). Projected changes in late-twenty-first-century tropical cyclone frequency in 13 coupled climate models from Phase 5 of the Coupled Model Intercomparison project. *Journal of Climate*, *26*(24), 9946–9959. <https://doi.org/10.1175/JCLI-D-13-00010.1>
- Vecchi, G. A., Delworth, T. L., Murakami, H., Underwood, S. D., Wittenberg, A. T., Zeng, F., et al. (2019). Tropical cyclone sensitivities to CO₂ doubling: Roles of atmospheric resolution, synoptic variability and background climate changes. *Climate Dynamics*, *53*(9–10), 5999–6033. <https://doi.org/10.1007/s00382-019-04913-y>
- Villarini, G., Lavers, D. A., Scoccimarro, E., Zhao, M., Wehner, M. F., Vecchi, G. A., et al. (2014). Sensitivity of tropical cyclone rainfall to idealized global-scale forcings. *Journal of Climate*, *27*(12), 4622–4641. <https://doi.org/10.1175/JCLI-D-13-00780.1>
- Walsh, K. J. E., McBride, J. L., Klotzbach, P. J., Balachandran, S., Camargo, S. J., Holland, G., et al. (2016). Tropical cyclones and climate change. *WIREs Climate Change*, *7*(1), 65–89. <https://doi.org/10.1002/wcc.371>
- Wehner, M., Reed, K. A., Stone, D., Collins, W. D., & Bacmeister, J. (2015). Resolution dependence of future tropical cyclone projections of CAM5.1 in the U.S. CLIVAR hurricane working group idealized configurations. *Journal of Climate*, *28*(10), 3905–3925. <https://doi.org/10.1175/JCLI-D-14-00311.1>
- Wehner, M. F., Reed, K. A., Loring, B., Stone, D., & Krishnan, H. (2018). Changes in tropical cyclones under stabilized 1.5 and 2.0°C global warming scenarios as simulated by the Community Atmospheric Model under the HAPPI protocols. *Earth System Dynamics*, *9*(1), 187–195. <https://doi.org/10.5194/esd-9-187-2018>
- Wright, D. B., Knutson, T. R., & Smith, J. A. (2015). Regional climate model projections of rainfall from U.S. landfalling tropical cyclones. *Climate Dynamics*, *45*(11–12), 3365–3379. <https://doi.org/10.1007/s00382-015-2544-y>
- Yamada, Y., Kodama, C., Satoh, M., Sugi, M., Roberts, M. J., Mizuta, R., et al. (2021). Evaluation of the contribution of tropical cyclone seeds to changes in tropical cyclone frequency due to global warming in high-resolution multi-model ensemble simulations. *Progress in Earth and Planetary Science*, *8*(1), 11. <https://doi.org/10.1186/s40645-020-00397-1>
- Yang, W., Hsieh, T. L., & Vecchi, G. A. (2021). Hurricane annual cycle controlled by both seeds and Genesis probability. *Proceedings of the National Academy of Sciences of the United States of America*, *118*(41), e2108397118. <https://doi.org/10.1073/pnas.2108397118>
- Yoshida, K., Sugi, M., Mizuta, R., Murakami, H., & Ishii, M. (2017). Future changes in tropical cyclone activity in high-resolution large-ensemble simulations. *Geophysical Research Letters*, *44*(19), 9910–9917. <https://doi.org/10.1002/2017GL075058>
- Yue, L., van de Lindt, J. W., Thang, D., Sigridur, B., & Aakash, A. (2012). Loss analysis for combined wind and surge in hurricanes. *Natural Hazards Review*, *13*, 1–10. [https://doi.org/10.1061/\(ASCE\)NH.1527-6996.0000058](https://doi.org/10.1061/(ASCE)NH.1527-6996.0000058)
- Zarzycki, C. M. (2016). Tropical cyclone intensity errors associated with lack of two-way ocean coupling in high-resolution global simulations. *Journal of Climate*, *29*(23), 8589–8610. <https://doi.org/10.1175/JCLI-D-16-0273.1>
- Zarzycki, C. M., & Ullrich, P. A. (2017). Assessing sensitivities in algorithmic detection of tropical cyclones in climate data. *Geophysical Research Letters*, *44*(2), 1141–1149. <https://doi.org/10.1002/2016GL071606>